Uğur YILDIZ

A Master's Thesis

AGU 2021

IMPROVING THE FLAME RETARDANCY USING NANOPARTICLES IN CABLE INSULATION

A THESIS
SUBMITTED TO THE DEPARTMENT OF
ADVANCED MATERIALS AND NANOTECHNOLOGY
AND THE GRADUATE SCHOOL OF ENGINEERING AND SCIENCE
OF ABDULLAH GUL UNIVERSITY
IN PARTIAL FULFILLMENT OF THE REQUIREMENTS
FOR THE DEGREE OF
MASTER OF SCIENCE

By
Uğur YILDIZ
June, 2021

IMPROVING THE FLAME RETARDANCY USING NANOPARTICLES IN CABLE INSULATION

A THESIS
SUBMITTED TO THE DEPARTMENT OF
ADVANCED MATERIALS AND NANOTECHNOLOGY
AND THE GRADUATE SCHOOL OF ENGINEERING AND SCIENCE OF
ABDULLAH GUL UNIVERSITY
IN PARTIAL FULFILLMENT OF THE REQUIREMENTS
FOR THE DEGREE OF
MASTER OF SCIENCE

By
Uğur YILDIZ
June, 2021

SCIENTIFIC ETHICS COMPLIANCE

I hereby declare that all information in this document has been obtained in accordance with academic rules and ethical conduct. I also declare that, as required by these rules and conduct, I have fully cited and referenced all materials and results that are not original to this work.

Uğur YILDIZ

REGULATORY COMPLIANCE

M.Sc. thesis titled **"Improving the flame retardancy using nanoparticles in cable insulation"** has been prepared in accordance with the Thesis Writing Guidelines of the Abdullah Gül University, Graduate School of Engineering & Science.

Prepared By	Advisor
Uğur YILDIZ	Asst. Prof. Ali DURAN

Head of the Advanced Materials and Nanotechnology Program

Prof. Murat DURANDURDU

ACCEPTANCE AND APPROVAL

M.Sc. thesis titled “Improving the flame retardancy using nanoparticles in cable insulation” and prepared by Uğur YILDIZ has been accepted by the jury in the Advanced Materials and Nanotechnology Graduate Program at Abdullah Gül University, Graduate School of Engineering & Science.

14 / 06 / 2021

JURY:

Advisor : Asst. Prof. Ali DURAN

Member : Prof. Niğmet UZAL

Member : Assoc. Prof. Erkan YILMAZ

APPROVAL:

The acceptance of this M.Sc. thesis has been approved by the decision of the Abdullah Gül University, Graduate School of Engineering & Science, Executive Board dated ….. /….. / …….. and numbered ……..…… .

…….. /…….. / ……..

(Date)

Graduate School Dean
Prof. Hakan USTA

ABSTRACT

IMPROVING THE FLAME RETARDANCY USING NANOPARTICLES IN CABLE INSULATION

Uğur YILDIZ
MSc. in Advanced Materials and Nanotechnology
Advisor: Asst. Prof. Ali DURAN

June, 2021

$Al(OH)_3$ (ATH) and $Mg(OH)_2$ (MDH) like materials are frequently used as flame retardants due to their ability to form water and oxide-based substances under the influence of heat. In this study, it is aimed to produce cable insulations with improved flame retardant properties by synthesizing nano-sized $Mg(OH)_2$ and using this material together with EVA (ethylene-vinyl-acetate) copolymer and micro-sized $Al(OH)_3$ and $Mg(OH)_2$.

The study can be divided into four parts. In the first part, the flame retardant properties of ATH and MDH were compared. In the second part, different raw materials were used for the synthesis of $Mg(OH)_2$ nanoparticles; in the third part, the synthesis was carried out at factory scale and compared with the commercial product. The samples were characterized by scanning electron microscopy (SEM), Fourier transform infrared spectrometer (FT-IR), X-Ray diffraction analysis (XRD), X-Ray fluorescence analysis (XRF) and Thermogravimetric analysis (TGA). In the last part, different amounts of nano-sized $Mg(OH)_2$ particles were added to the formulas using both ATH and MDH; the effects on flame retardant performances were investigated by the Limiting Oxygen Index (LOI) test and the vertical burning test. Mechanical properties such as elongation and tensile strength were also studied.

It has been observed that the synthesized $Mg(OH)_2$ particles with a thickness of 5-10 nm and lengths reaching 900 nm, mixed in ATH based samples at a maximum rate of 9% and in MDH based samples at a maximum rate of 10%; LOI values increased by 26% for ATH based samples and 38% for MDH based samples. However, considering the losses in mechanical properties with the increase of nanoparticle additive, it has been seen that a maximum rate of 5% nano-sized $Mg(OH)_2$ can be added. Even in this case, the LOI values increased by 8.6% in ATH based samples and 26% in MDH based samples.

Keywords: Flame Retardancy, Cable Insulation, $Mg(OH)_2$ nanoparticle, EVA copolymer

ÖZET

KABLO İZOLASYONUNDA NANOPARTİKÜLLER KULLANILARAK ALEV GECİKTİRİCİ ÖZELLİĞİN GELİŞTİRİLMESİ

Uğur YILDIZ
İleri Malzemeler ve Nanoteknoloji Anabilim Dalı Yüksek Lisans
Tez Yöneticisi: Dr. Öğr. Üyesi Ali DURAN
Haziran, 2021

$Al(OH)_3$ (ATH) ve $Mg(OH)_2$ (MDH) gibi maddeler, ısı etkisi altında su ve oksit bazlı madde oluşturma kabiliyetleri nedeniyle alev geciktirici olarak yaygın bir şekilde kullanılmaktadırlar. Bu çalışmada, nano boyutta $Mg(OH)_2$ sentezlenerek, bu maddenin EVA (etilen-vinil-asetat) kopolimeri ve mikro boyutta $Al(OH)_3$ ve $Mg(OH)_2$ ile birlikte kullanılması ile alev geciktirici özellikleri geliştirilmiş kablo izolasyonları üretilmesi amaçlanmıştır.

Çalışma dört bölüme ayrılabilir. Birinci bölümde ATH ve MDH'nin alev geciktirici özellikleri karşılaştırılmıştır. İkinci bölümde, $Mg(OH)_2$ nanopartikülleri farklı hammaddeler kullanılarak sentezlenmiştir. Üçüncü bölümde sentez, fabrika boyutunda yapılmış ve ticari ürün ile karşılaştırılmıştır. Örnekler, taramalı elektron mikroskobu (SEM), Fourier dönüşümü kızılötesi spektrometresi (FT-IR), X-Işını difraktometresi (XRD), X-Işını floresans spektrometresi (XRF) ve Termogravimetrik analiz (TGA) ile karakterize edilmiştir. Son bölümde, ATH ve MDH kullanılan formüllere farklı miktarlarda nano boyutlu $Mg(OH)_2$ partikülleri eklenmiş; Limit Oksijen İndeksi (LOI) testi ve dikey yanma testi ile alev geciktirici performansları üzerindeki etkileri araştırılmıştır. Uzama ve çekme dayanımı gibi mekanik özellikler de incelenmiştir.

ATH bazlı numunelerde maksimum %9, MDH bazlı numunelerde maksimum %10 oranında karıştırılan, 5-10 nm kalınlıkta ve yer yer uzunlukları 900 nm'ye ulaşan $Mg(OH)_2$ partikülleri LOI değerleri; ATH bazlı numuneler için %26 ve MDH bazlı numuneler için %38 oranında artmıştır. Ancak nanopartikül katkısının artmasıyla mekanik özelliklerde yaşanan kayıplar dikkate alındığında, maksimum %5 oranda nano boyutlu $Mg(OH)_2$ eklenebileceği görülmüştür. Bu durumda bile LOI değerleri ATH bazlı örneklerde %8,6 iken MDH bazlı örneklerde %26 oranında artmıştır.

Anahtar kelimeler: Alev Geciktirici, Kablo İzolasyonu, $Mg(OH)_2$ nanomalzeme, EVA kopolimer

Acknowledgements

First of all, I would like to express my deepest gratitude to my supervisor Asst. Prof. Ali DURAN for his unlimited support, invaluable advice, guidance, encouragement and valuable hours he spent in completing my thesis. His industry-oriented thinking in every work I did during my graduate education has provided me an incredible benefit both in my business life and in my university life.

I'd like to express my gratitude to Asst. Prof. İlker ERDEM, who benefited from all of his knowledge during my studies and supported me with his help and comments in the characterizations we applied.

I would also like to thank Prof. Ertuğrul ŞEHMETLİOĞLU, Assoc. Prof. M. Serdar ÖNSES and Assoc. Prof. Erkan YILMAZ from Erciyes University Nanotechnology Research Center (ERNAM) for their guidance in my research and knowledge that I have benefited from.

I sincerely thank to my colleagues in my workplace Hes Kablo, to head of R&D department Mahmut Akif NURSAÇAN, to my most important assistant in the production process of samples Ahmet SARISOY, to R&D engineer Ali ÖZÇUKURLU for his valuable assistance, to Laboratory engineer Ayşenur FIRAT and R&D engineer Aybike ERDENİZ for their support in characterization of the samples.

I want to thank my managers at Hes Kablo, whose names I have not mentioned here, for the convenience and support they provided in making use of all the facilities of the facility throughout my thesis.

Finally, I'd like to express my special thanks to my family and my dear wife Raziye YILDIZ because of her infinite patience, self-sacrifice to help my work, love, understanding and encouragement; to my dear son Nezir Beslan for the extra encouragement he gave me with his understanding and cuteness while working.

Table of Contents

List of Figures

List of Tables

List of Abbreviations

ATH	Aluminum Trihydroxide
DTA	Differential Thermal Analysis
EDX	Energy-Dispersive X-ray Spectroscopy
EPR	Ethylene Propylene Rubber
ERNAM	Erciyes University Nanotechnology Research Center
EVA	Ethylene Vinyl Acetate
FT-IR	Fourier-Transform Infrared Spectroscopy
HFFR	Halogen Free Flame Retardant
LOI	Limiting Oxygen Index
MDH	Magnesium Dihydroxide
PE	Polyethylene
PU	Polyurethane
PVC	Polyvinyl Chloride
SEM	Scanning Electron Microscopy
TGA	Thermogravimetric Analysis
VA	Vinyl Acetate
XLPE	Cross-Linked Polyethylene
XRD	X-ray Diffraction
XRF	X-ray Fluorescence

To my dad

Chapter 1

1. Introduction

Nowadays polymer materials find wide use in every aspect of life. These wide areas of use also bring some dangers with it. Fire risk is the biggest problem due to the flammable characteristics of polymer materials. At this point, the use of flame retardants allows the reduction of flammability and the reduction of smoke and toxic gas production [1]. Each year in Turkey, electrical fires take second place in the causes of fire occurrence [2]. Hidden in construction, kilometers of cables contain tons of polymer. Even the fire is not caused by cables, they create a great effect on the spreading of the fire because of this polymer content [3]. The use of flame retardant cables in buildings has begun to be a requirement, thanks to emphasis of governments on this issue. The main purpose of using these cables is to delay the spreading of the fire and to give people the time they need to evacuate the building. In the main time, halogen-based flame retardants (like Br, Cl) to be used threaten human health due to the toxic gases they emit. For this reason, halogen free flame retardants (HFFR) are used as the main flame retardants in cables. Aluminum hydroxide (ATH) and magnesium hydroxide (MDH) hydrated minerals are the main HFFRs used in cable insulation because of low cost and easy processibility. When ATH and MDH interact with heat, they release water by decomposition as a result of an endothermic reaction. For ATH, this temperature is around 220^{o}C while for MDH it is around 330^{o}C. Metal oxides Al_2O_3 and MgO, formed as a result of decomposition of ATH and MDH, form a char layer on the polymer surface and isolate is from heat and oxygen. Particle size, shape and distribution, chemical purity, particle shape and surface area parameters play an important role for these minerals. The only limiting factor in the use of these materials is the high usage requirements to be effective. Therefore, the polymer to be used as a carrier gains great importance. Ethylene vinyl acetate (EVA) is an excellent polymer because of its mechanical and physical properties widely used in cable industry [4]. Besides its easy processability, it is preferred in extrusion processes due to its ability to carry up to 65% filler material by weight [5]. On the other hand, high filling content

increases the losses in mechanical properties. In order to increase the effectiveness of hydrated minerals, many studies have been published where new formulas created by substituting partially these minerals with some additives [6] like expandable graphite [7], zinc borate [8], carbon nanotubes [9]. Also, in some studies it was shown that MDH nano particles are used to improve the fire performance [10].

In this study, nano-scale MDH particles synthesized and used in combination with different flame retardants to improve the flame retardant property. Although there are many studies about nano-sized MDH synthesis and its effect on flame retardancy, most of them limited with laboratory studies. As far as we know, there is no data on the production of nano MDH based products on a factory scale and its actual use in production. This study was carried out in four main parts. In the first part compound samples were prepared by formulating ATH, synthetic MDH and natural MDH flame retardants with EVA polymer in order to compare their flame retardant properties. Another purpose aimed with the use of natural and synthetic MDH here is to monitor the effect of both grain size and purity on flame retardancy. ATH is the main flame retardant additive used in flame resistant cables in Hes Kablo, so a comparison has been made with it. All flame retardants were characterized by using Fourier transform infrared spectroscopy (FT-IR), and their burning performance was compared with the vertical combustion test. In the second part, MDH synthesis was carried out at laboratory scale by using $MgCl_2$, $Mg(NO_3)_2$ and $MgSO_4$ mineral salts. The products have been characterized using scanning electron microscopy (SEM), Mg contents and unit prices of the minerals were compared for factory size production. In the third part, a 200 L capacity reactor produced in Hes Kablo for factory-scale production. Comparison of the nano-sized synthesized MDH and the micro-sized commercial MDH product was made. The products were characterized by using scanning electron microscopy (SEM), Energy-Dispersive X-ray Spectroscopy (EDX), X-ray Diffraction (XRD), Thermogravimetric (TGA) Analysis and Fourier-Transform Infrared Spectroscopy (FT-IR). In the fourth part, the formulations were formed with EVA polymer by mixing the synthesized nanoscale MDH with ATH and commercial MDH at various ratios. All of the products were characterized by Fourier-Transform Infrared Spectroscopy (FT-IR) and Limiting Oxygen Index (LOI) values were measured. As a result, a high flame retardant cable insulation was produced with the addition of nano-sized MDH that can be produced in the factory environment without increasing production costs.

Chapter 2

2. Literature review

2.1 Electrical Cables

An electrical cable is used to carry electric current. It is a combination of bundled or running side by side one or more wires. A typical cable diagram is given in Figure 2.1.

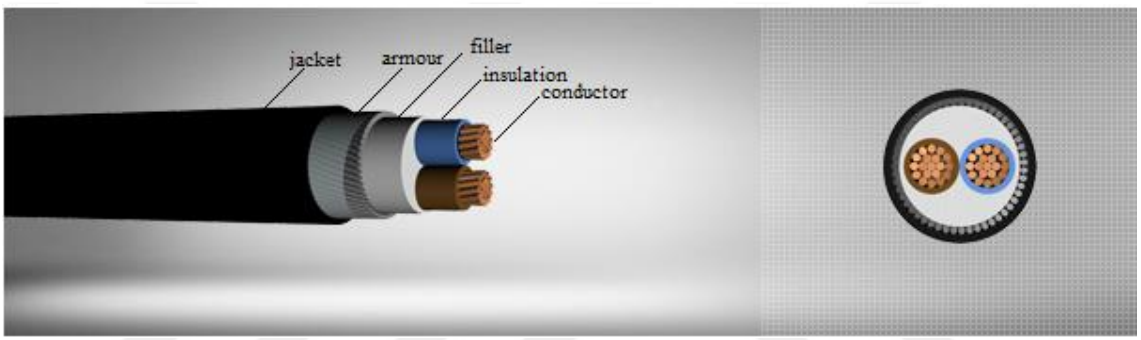

Figure 2.1 Electrical cable diagram [11]

Elements which build the cable are:

- **Conductor**: It moves the electric current and consist of a combination of one or more metallic threads.
- **Insulation**: It prevents the outflow of electricity by covering the conductor.
- **Fill layer**: It is an insulating material that keeps the whole circular section by surrounding the conductors.
- **Cover, jacket**: It is generally made of polymeric material and provides mechanical protection for the conductor against the action of temperature, rain, sun, etc.

- **Protection**: In some cases, the cable can carry a metal shield or a screen. This provides isolation to the signals from external interference or it can be an armor for mechanical protection against external aggression [12].

2.1.1 Electrical Cable Types

Cables can be classified under many headings. They can be classified according to their usage areas as given in Figure 2.2.

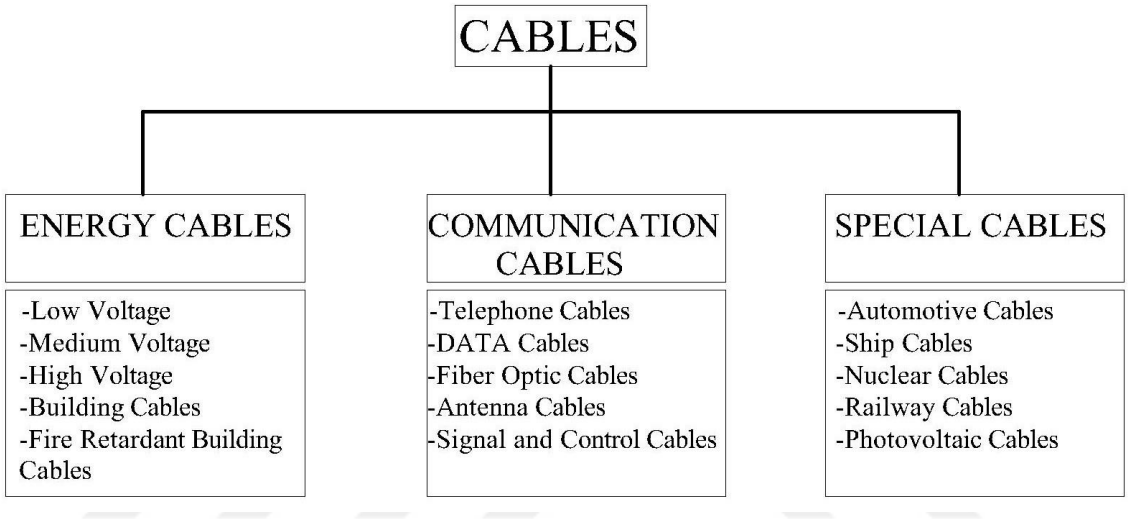

Figure 2.2 Electrical cable types according to usage areas

2.1.2 Insulation Types of Cables

Insulation is a dielectric material or can be define as a material resistant to the flow of electric current. Insulation resists electrical leakage, prevents the wire's current from coming into contact with other conductors. It preserves the material integrity of the wire by protecting against environmental threats such as water and heat. Insulation is the basis of the safety and effectiveness of the wire. Insulation materials are classified into two large groups: thermoplastic and thermoset as given Figure 2.3 [13].

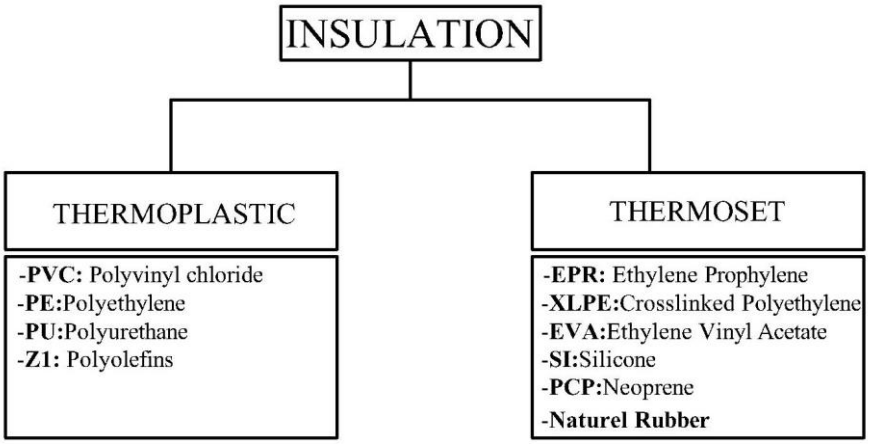

Figure 2.3 Insulation Types of Cables

2.1.2.1 Thermoplastic Materials

Thermoplastic materials are softened as they are heated and hardened when they cooled. **PVC (Polyvinyl Chloride):** Because of its low cost, durability and widely available properties, PVC is the most commonly used thermoplastic insulator for cables. However, PVC contains chlorine (halogen) in it and when PVC burnt, a thick, toxic and black smoke occurs. This smoke can be a health hazard in areas where low smoke and toxicity are required. (for example, tunnels) Operating temperatures are between 75ºC and 105 ºC (depending on PVC type) [14]. Chemical formula of PVC is given in Figure 2.4

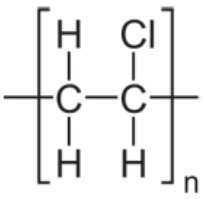

Figure 2.4 Chemical formula of PVC

PE(Polyethylene): Polyethylene has a low dielectric constant and stable dielectric constant over all frequencies. polyethylene can range from very soft to very hard depending on molecular weight and density in terms of flexibility. The most flexible has the lowest density and hardest has high density and high molecular weights. Moisture resistance of PE is excellent, however, both types are flammable [15]. Chemical formula of PVC is given in Figure 2.5

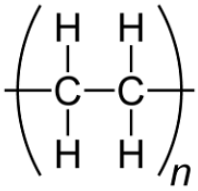

Figure 2.5 Chemical formula of PE

2.1.2.2 Thermoset Materials

Thermoset materials are not soft, flow or distort when they heated or pressurized. These compounds are not re-melt after heat treatment; however, they can be burnt or deteriorate due to heat.

XLPE (Cross-Linked Polyethylene): It is a material, formed by combination of different polyethylene chains linked together. At elevated temperatures it provides a prevention to the material from melting or separating. Crosslinks take place with a help of an agent like dicumyl peroxide [16].

EPR (Ethylene Propylene Rubber): EPR, sometimes called EPM is commonly called an elastomer, is a copolymer of polyethylene and propylene. Flexibility is higher than PE and XLPE besides dielectric losses are higher also. Normal operating temperatures are between 90^{o}C and 110^{o}C. The skeletal formula of EPR is given in Figure 2.6.

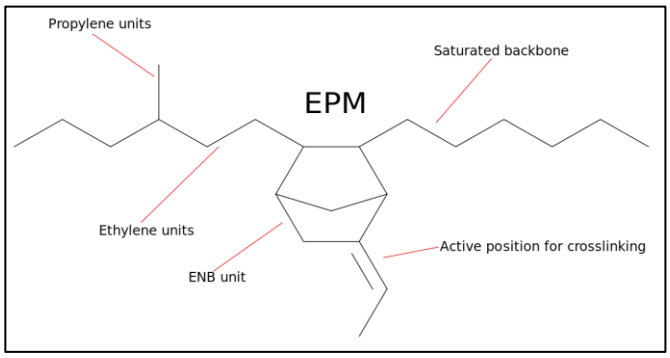

Figure 2.6 The skeletal formula of ethylene propylene rubber [17]

In Table 2.1, advantages and disadvantages of insulating materials are compared.

Table 2.1 Advantages and disadvantages of insulating materials

Material	Advantages	Disadvantages
PVC	*Cheap *Durable *Widely available	*Highest dielectric losses *Melts at high temperatures *Contains halogens *Not suitable for MV/HV cables
PE	*Lowest dielectric losses *High initial dielectric strength	*Highly sensitive to water treeing *Material breaks down at high temperatures
XLPE	*Low dielectric losses *Improved material properties at high temperatures *Does not melt but thermal expansion occur	*Medium sensitivity to water treeing (although some XLPE polymers are water-tree resistant)
EPR	*Increased flexibility *Reduced thermal expansion (relative to XLPE) *Low sensitivity to water treeing	*Medium-high dielectric losses *Requires inorganic filler/additive

2.1.3 Cable Production

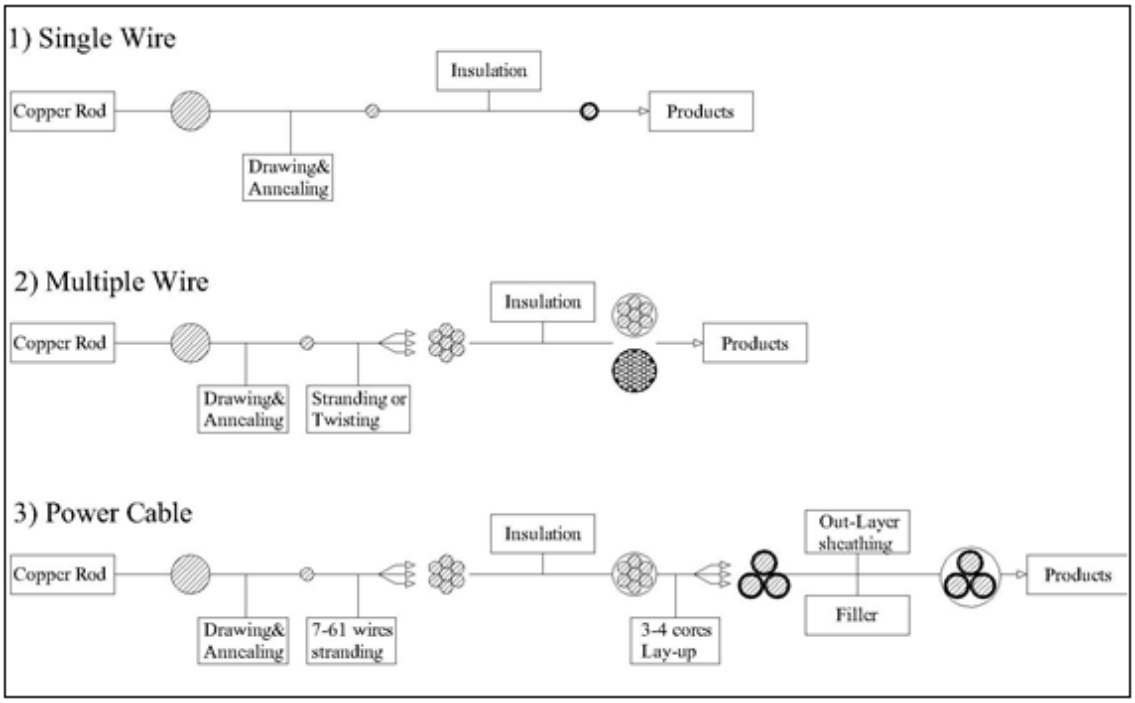

Figure 2.7 Some type of cable manufacturing diagrams [18]

Some type of cable manufacturing diagrams are given in Figure 2.7, according to the number of wires and their combined forms.

2.1.3.1 Wire Drawing

Copper or aluminum rod is brought to the desired diameter value on draw bench, by pulling through a series of synthetic diamond dies, which gradually decrease in size. While performing this process, a cooling and lubricating system is used to prevent the wire from overheating and increase the life of dies. In Figure 2.8, mechanism of drawing process is given, Figure 2.9 a wire drawing die sketch is shown.

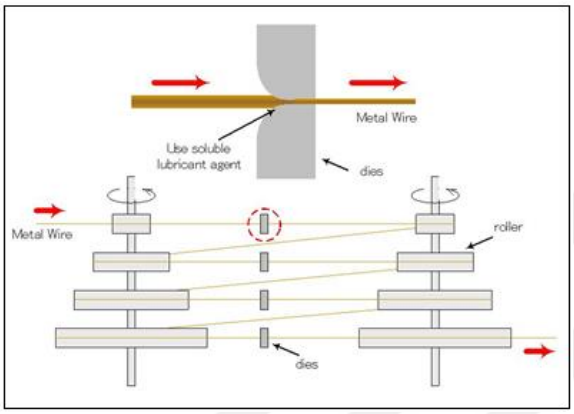

Figure 2.8 Mechanism of drawing process [19]

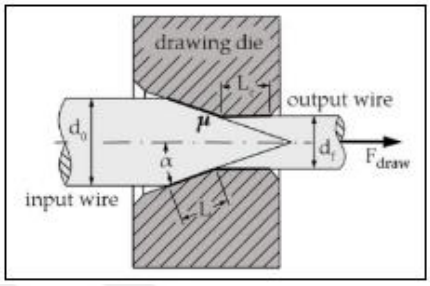

Figure 2.9 Wire drawing die [20]

2.1.3.2 Annealing

During the drawing process, a tremendous pressure is being applied on metal rod to form a thinner wire. Thus, the resulting wire is extremely fragile and can easily break if stretched. The elongation value of the wire has decreased to 1-3%. The finished wire must be flexible, therefore, the wire must be softened and annealed.

By heating the wire to its recrystallization temperature for a period of time, annealing is being accomplished. The key here is to avoid oxidation of the wire. So that reason, protective atmospheres are being used like vapor or nitrogen. A basic process scheme is given in Figure 2.10.

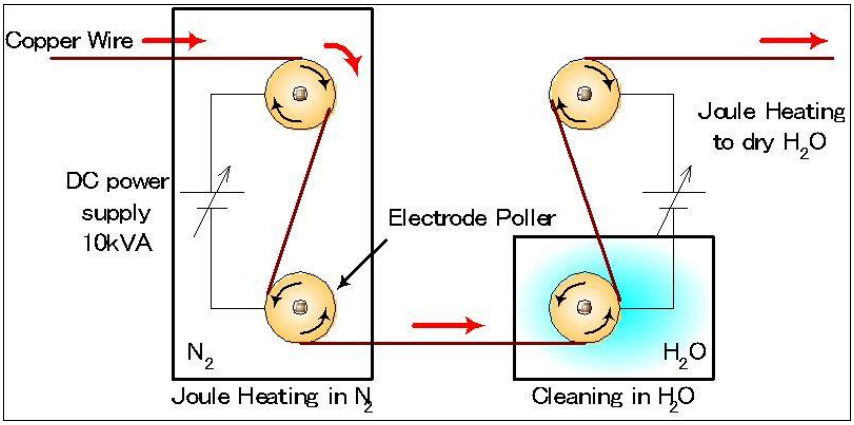

Figure 2.10 Annealing and cleaning process [19]

2.1.3.3 Twisting and Stranding

Two or more wires of the same gauge are twisted or stranded together to achieve better flexibility and electrical performance. To determine exact twist length, a proprietary formula is being used. In Figure 2.11 wire twisting schema and stranding process figure are given.

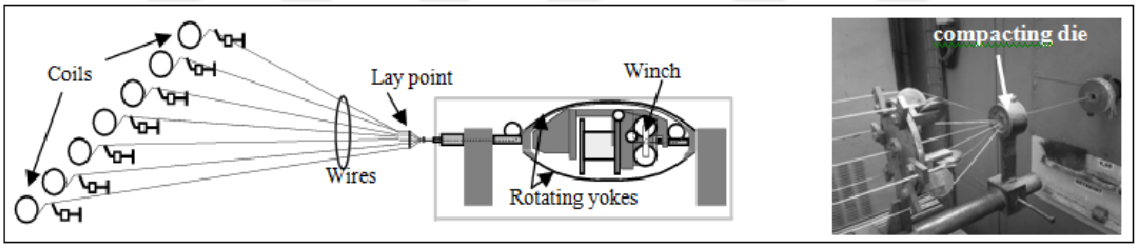

Figure 2.11 Wire twisting and stranding process [21]

2.1.3.4 Extrusion

2.1.3.4.1 Compound Extrusion

Before cable was produced, the compound is produced in an extruder. The process of melting the polymer and mixing with additives, e.g., fillers or reinforcing materials, called compounding. By the help of this process, the physical, thermal, electrical or aesthetic properties (conductivity, flame resistance, wear resistance, color etc.) of the polymer are changed. The final product is called a compound [22].

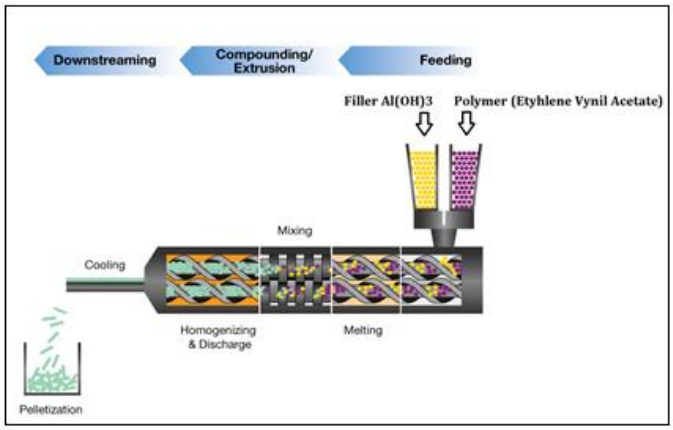

Figure 2.12 Compound extrusion process [23]

Filler and polymer add to the extruder with help of gravimetric feeders. Fillers are added to polymers to improve their properties and/or reduce the price of the compound. A wide variety of applications use fillers in the polymer matrix for good incorporation options. The materials enter from the hopper into the feed throat. The rotary motion of screw conveys the entered materials. The solid polymer is converted into the melt with mechanical shear from the screw and thermal heat from the barrel, then pushed out of the die. After the compound has cooled, a knife cuts it into small granules. (Figure 2.12)

2.1.3.4.2 Cable Extrusion

There are 5 different components of a simple extrusion line which are pay-off, extruder, cooling shaft/curing shaft, capstan (pulling device) and take-up as shown in Figure 2.13.

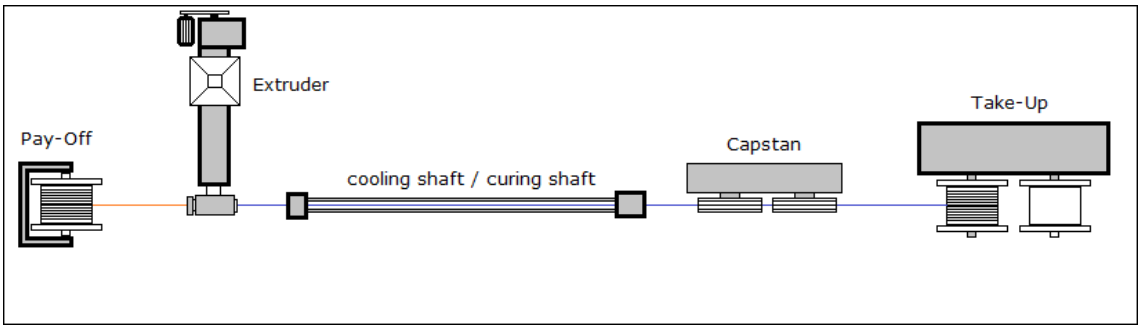

Figure 2.13 Basic extrusion line [24]

This line is enough to coat desired wire with plastic, but for good quality and higher volume of production there must be additional units. Common auxiliary units

are preheater, feeding and take up accumulator, powdering unit, tape applicator, spark tester, in-line diameter gauge.

2.1.3.4.2.1 Pay-Off

Pay-off unit can be loaded with wire or cable conductor to be coated. It feeds the extrusion line. It can be work with a flyer (Figure 2.15) or can be motor driven (Figure 2.14) with accumulator for high-speed extrusion. Bobbin size also important to determine the type of the pay-off unit. Final product type and line speed determine the pay-off selection.

Figure 2.14 Motor driven pay-off [25]

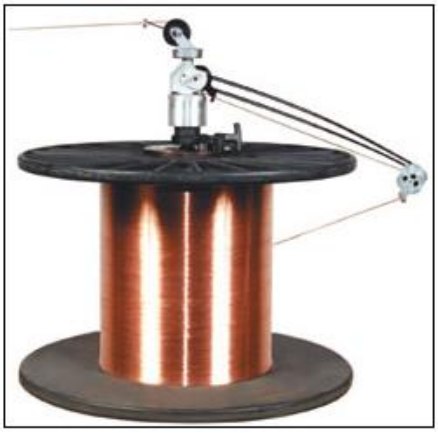

Figure 2.15 Flyer type pay-off [26]

2.1.3.4.2.2 Extruder

Main unit of extrusion line is extruder. It forms the plastic is formed and coats over bare conductor. A simple extruder model and image are given in Figure 2.16.

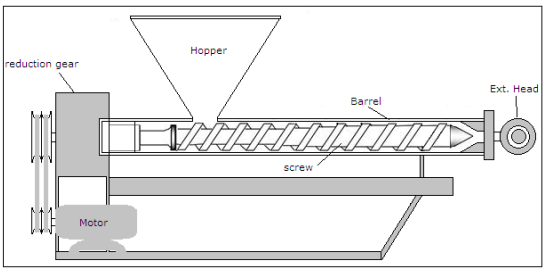

Figure 2.16 Cable extruder [27]

By means of rotating screw in the barrel; plastic is pushed to extrusion head where it would be coated and formed. There are many types of barrel and screws depends on physical aspects of extruded plastic.

2.1.3.4.2.3 Cooling Shaft

After extrusion process, thermoplastic coated cable should be cooled down. A cooling shaft is full of water where extruded cable will go through. Water in cooling shaft is would be warmed up. In order to maintain a stable temperature; water needs to be cooled. Dimensions of cooling shaft would be determined by minimum and maximum cable size, line speed, ambient temperature and water tank capacity.

2.1.3.4.2.4 Curing Shaft

Thermoset plastics extruded as cold forming. After extrusion process, plastic needs to be cured. According to the type of extruded plastic, curing heat and using of gases can be variable. Curing unit dimensions would be determined by line-speed, desired temperature and physical characteristics of the plastic material.

2.1.3.4.2.5 Capstan (pulling)

Capstan pulls the extruded cable through extrusion process and cooling/curing shaft then feeds take-up unit as given in Figure 2.17. Capstan speed over extruder speed ratio determines the final dimensions of the product. The line speed determines by capstan's pulling speed and pulling force. A capstan is simply accoupled pulleys. Pulleys can be positioned vertical, horizontal or belted. Belted capstan, also known as "caterpillar" (Figure 2.18).

Figure 2.17 Capstan [28]

Figure 2.18 Caterpillar [29]

2.1.3.4.2.6 Take-up

It is the end point of an extrusion line. It can be work with a single or double spool and manual or automatic change. The size of take-up is determined by size of the spool, size of cable and line speed. A traverse unit must be on it for proper winding. For arranging the winding speed, a dancer or accumulator unit required in front of take-up unit. A type of take-up machine is given in Figure 2.19.

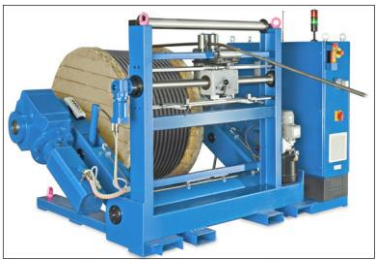

Figure 2.19 Take-up machine [30]

2.1.4 Fire Retardant Cables

Fire is one of the disasters we can encounter in our lives at any moment. Each of the electrical devices we use can actually be a cause of fire. To minimize vital risks, there are three important points about fire.

1. Taking measures to prevent the occurrence of fire
2. Taking measures to prevent the growth of fire.
3. Fastest extinguishing of fire.

An example for item 1, the chemicals used in the facilities can be stored in separate sections and classes, for item 2, the use of fire retardants in the materials used, and for item 3 the establishment of appropriate fire extinguishing systems where there is a risk of fire can be given. This study will focus on item 2, solutions will make people more time to escape by delaying the formation of the fire will be searched.

In case of a fire, electricity transmission to elevators, ventilation devices, emergency warning lights etc. must be uninterrupted to provide saving time for people to escape. In addition, considering that the polymer used in these cables will burn, it should

not create impressive smoke and toxic gases for human health. Therefore, the use of cables with flame retardant additive is an inevitable necessity for high buildings, shopping malls, cinemas, train stations, planes etc.

2.1.4.1 Formation of Fire

Three elements are needed to ignite the fire; heat, fuel and oxygen. Removing or partially blocking one of them prevents or slows fire formation.

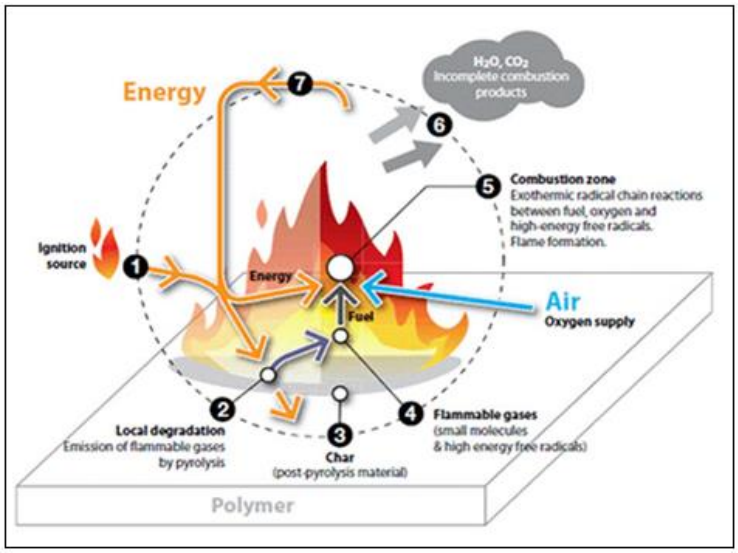

Figure 2.20 Formation of fire [31]

As given in Figure 2.20, when polymers burn, they form large amounts of free radicals. These free radicals combine with oxygen in the air to cause combustion to continue. Combustion creates energy and this energy works as an ignition source and allows the combustion to continue until the polymer run out.

2.1.4.2 Flame Retardance Mechanisms in Plastics

2.1.4.2.1 Vapor Phase Inhibition (Halogen Based Flame Retardants)

During combustion, flame retardant additives react with the burning polymer in the vapor phase. They disrupt the production of free radicals and shuts down the combustion process. (Figure 2.21) Halogenated flame retardant systems commonly use this

mechanism as given in Figure 2.22 (Especially Br, Cl). However, halogen-based flame retardants may generate harmful gases during combustion.

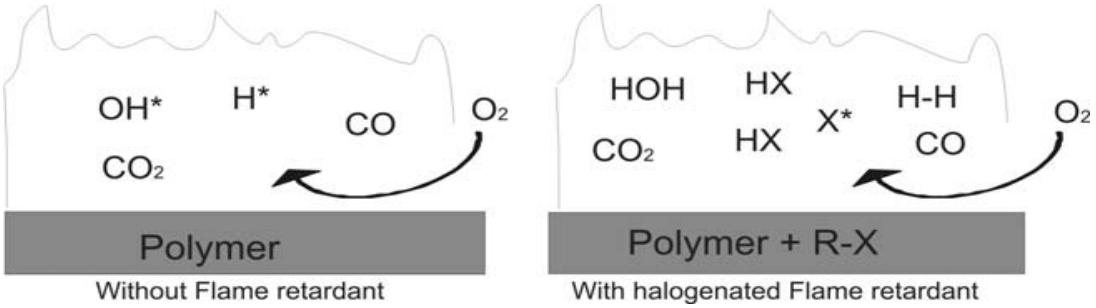

Figure 2.21 Radical formation with and without halogenated FR additives [32]

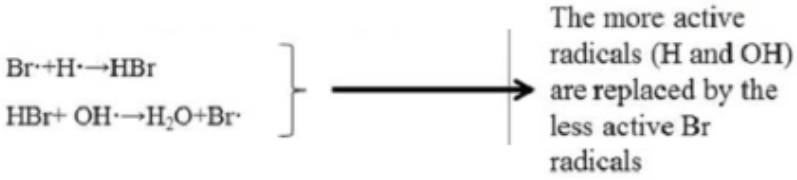

Figure 2.22 Brominated flame retardant working mechanism [33]

2.1.4.2.2 Solid Phase Char-Formation (Phosphorous Based Flame Retardants)

On the material's surface a carbonaceous layer is formed with the reaction of char-forming flame retardant additives. With the help of this layer a barrier is created which insulates the polymer, slows pyrolysis and hinders the release of additional gases to fuel combustion (Figure 2.23). Non-halogen systems using phosphorous and nitrogen chemistries commonly prefer this method (Figure 2.24) [34].

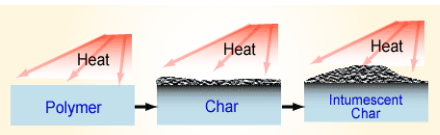

Figure 2.23 Char-formation [35]

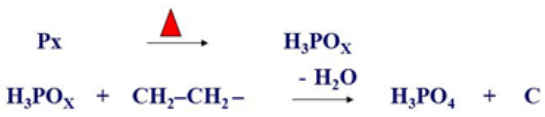

Figure 2.24 Phosphorous FR working mechanism [36]

2.1.4.2.3 Quench&Cool

This method used mostly for extruded applications like wire and cable. The additives are hydrated inorganic minerals like aluminium trihydroxide, magnesium hydroxide. In these systems, an endothermic reaction occurs at the time of contact with fire and water molecules are released which cool the polymer (Figure 2.25) [34].

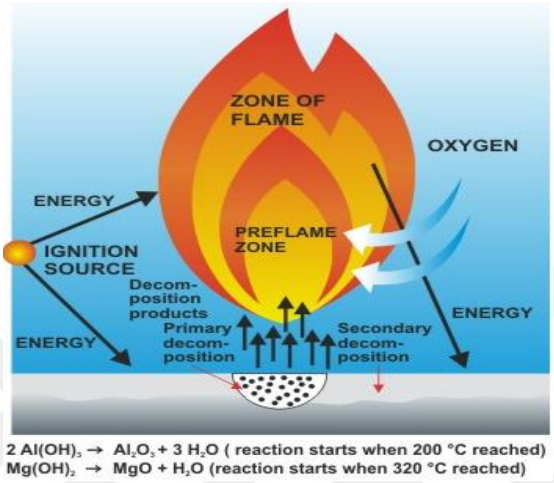

Figure 2.25 Quench&cool mechanism [35]

2.1.4.3 Halogen Free Flame Retardant (HFFR) Cable Production

Before producing cable, the compound is produced. As given in Figure 2.26, filler ($Al(OH)_3$) and polymer add to the extruder. In extruder polymer melts down, it mixes with the filler powder. After the compound has cooled, a knife cuts it into small granules.

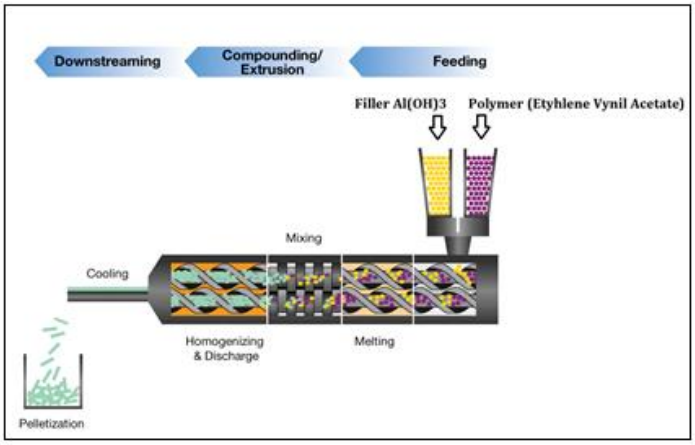

Figure 2.26 Compound production of HFFR cable [23]

This compound is added to the cable extruder. It is melted again and pushed to the coating mold. The copper wire enters the mold and is insulated. A model of cable extruder is given in Figure 2.27.

Figure 2.27 Cable extruder [37]

Below in Table 2.2 shows the components and their ratios in formula.

Table 2.2 Ratios of compound elements in formula

Component	Quantity (%)
EVA (Ethylene Vinyl Acetate)	30
Al $(OH)_3$	60
Additives (coupling agent, antioxidant etc.)	10

2.1.4.4 EVA Copolymer

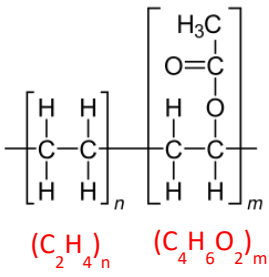

Polyethylene - vinyl acetate

Figure 2.28 Chemical formula of EVA [38]

Table 2.3 Effect of VA%ratio to melting point [39]

VA%	Melt Point (°C)
40	47
32	63
28	75
25	78
18	88
12	96
9	100
0	110

Ethylene vinyl acetate (EVA) is a copolymer of ethylene and vinyl acetate with a structure as shown in Figure 2.28. EVA copolymers containing about 10 and 30 percent vinyl acetate are used for a myriad of applications. Important applications include sealants in meat and dairy packaging structures, footwear, wire and cable insulation, pipes, toys, corks, photovoltaic encapsulation, medical packaging, hot melt adhesives, and lamination of glass to improve impact resistance [40]. Vinyl acetate additive effects melting point and flexibility of polymer. (Table 2.3) The flexibility is important for cables because there mustn't be any cracks on the cable when it is bended or when exposed to sunlight for a long time.

2.1.5 Flame Retardancy Mechanism of Magnesium Hydroxide

When $Mg(OH)_2$ heated in 320℃, it decomposes as equation 2.1;

$$Mg(OH)_2 \rightarrow MgO + H_2O \qquad \Delta H = -328\ cal/g \tag{2.1}$$

Same reaction for $Al(OH)_3$ starts at 200 ℃ as equation 2.2,

$$2Al(OH)_3 \rightarrow Al_2O_3 + 3H_2O \qquad \Delta H = -230\ cal/g \tag{2.2}$$

It releases large quantities of moisture to attenuate oxygen gas on the surface of polymer. After the above reaction, magnesium oxide will be generated. This magnesium oxide sticks to surface of polymer, it can further prevent burning. Because the melting point of MgO is 2.852 °C. Also, during the whole inflaming retarding process, not only it won't produce any hazardous substance, but also it can absorb large amounts of smoke and noxious gas produced by burning plastics [41].

2.1.6 Determination of Flame Retardancy

2.1.6.1 Limiting Oxygen Index (LOI)

It is one of the critical indicators of flame retardancy. It means that, the minimum percentage of oxygen that need for the combustion of a polymer.

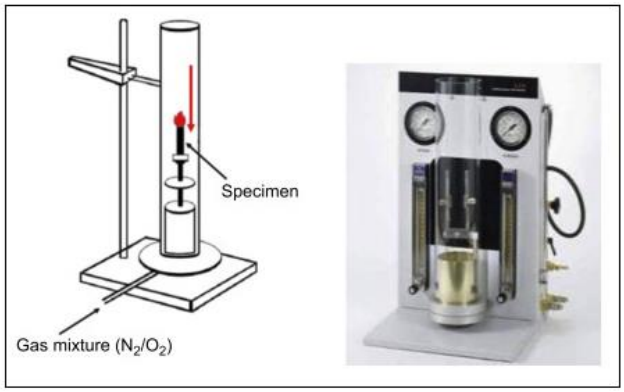

Figure 2.29 Schematic drawing and instrument of LOI test [42]

In the LOI test a candle-like sample is supported in a vertical glass column and a slow stream of oxygen/nitrogen mix is fed into the glass column. A flame ignites the sample and it burns downward into unheated material. The oxygen/nitrogen ratio can be varied and the test records the minimum concentration of oxygen (as a percentage) that will just support combustion. (Figure 2.29) The LOI test is a basic property of the material, but it cannot give any clue about how the material will react during burning in an open atmosphere [43].

Air contains 21% oxygen. Standard PU foam needs 16.5% oxygen for combustion. That means when PU foam is ignited, it burns until foam is ended. But as shown in Table 2.4., PTFE needs 95% of oxygen. That means it cannot be ignited in atmospheric environment.

Table 2.4 LOI values of some polymers

Some Typical Values	**LOI (%)**
Std Polyurethane foam	16.5
PMMA (Perspex)	17.3
Poly(ethylene)	17.4
Poly(propylene)	17.4
Poly(styrene)	17.8
Plywood	23.0
Nylon 6.6	24-29
Polycarbonate	25-44
Nomex	28.5
Polyester (GRP)	21-43
Phenolic	26-64
PVC (unplasticized)	45-49
PTFE	95

2.1.6.2 Vertical Flame Test

This test is based on measuring of the time-dependent spread of the flame as shown in Figure 2.30 [44].

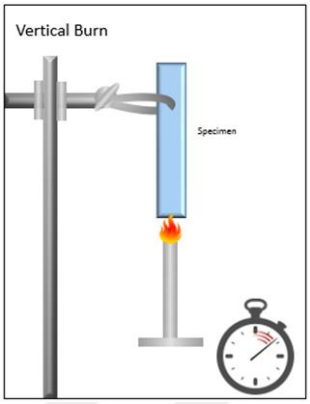

Figure 2.30 Vertical flame test set-up

Chapter 3

3. Materials and Methods

3.1 Chemicals

All the chemicals used in the experiments were; magnesium chloride ($MgCl_2$, Maltaş, Turkey), magnesium sulphate ($MgSO_4$, Maltaş, Turkey), magnesium nitrate ($Mg(NO_3)_2$, Maltaş, Turkey), ammonia (NH_3 25% Tekkim, Turkey), magnesium hydroxide ($Mg(OH)_2$, Magnifin, Germany), Brucite (($Mg(OH)_2$, Nuova Sima, Italy), aluminum hydroxide($Al(OH)_3$, ETİ, Turkey), hydrochloric acid (HCl, Merck, Germany)

3.2 Polymers

The polymers used in the experiments; ethylene vinyl acetate (EVA) (28% vinyl acetate ratio), EVA (48% vinyl acetate ratio) supplied from Hes Kablo Inc. (Kayseri, Turkey)

3.3 Equipments

3.3.1 Nano-scale Particle Synthesis Set-up

For lab-scale production (20 L solution capacity), ERNAM (Erciyes University Nanotechnology Research Center) polymer laboratory is used. In Figure 3.1, lab-scale nanoparticle synthesis set-up is shown.

Figure 3.1 Lab-scale nanoparticle synthesis set-up

For factory scale production (200 L solution capacity), a reactor is designed and built in Hes Kablo. (Figure 3.2) 200 L capacity metal barrel covered with a jacket-resistant to achieve desired temperature. A temperature control device and a thermocouple added to set exact temperature. Maximum temperature is 80^{o}C.

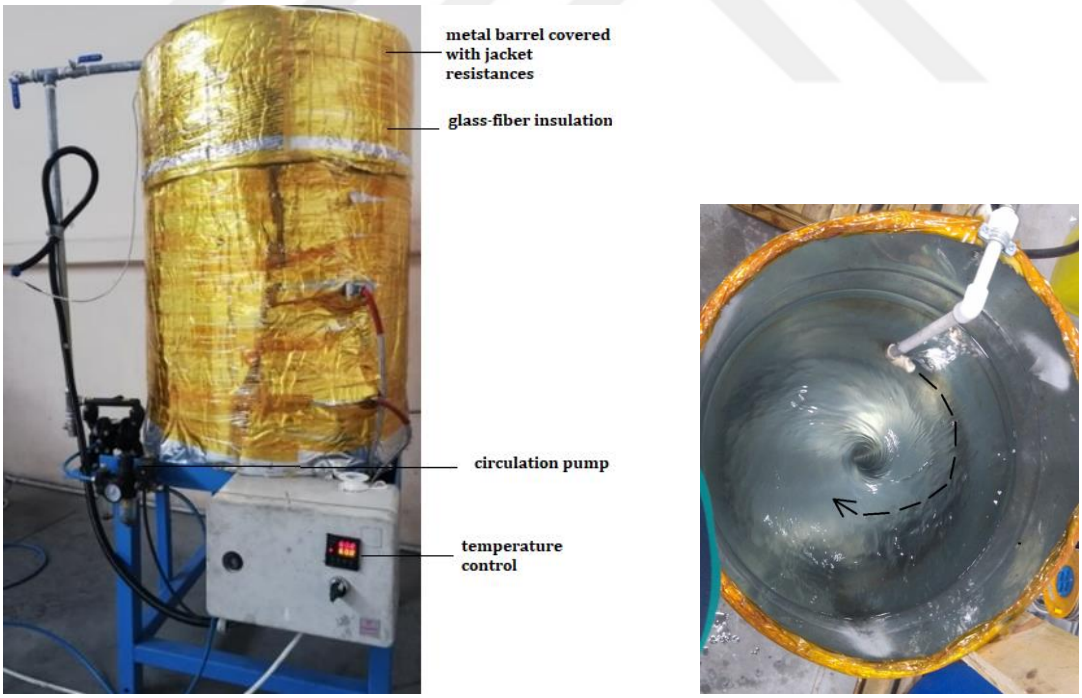

Figure 3.2 Factory-scale nanoparticle synthesis set-up

Circulation pump is circulating the solution with a capacity of 40 l/min. To create a more homogeneous solution, the end of discharge pipe of pump oriented at a horizontal angle as given in Figure 3.2.

3.3.2 Extruders

Two types of extruders are used for the experiments. First extruder is the Gülnar (Kayseri, Turkey) brand extruder that is in ERNAM Polymer Laboratory (Figure 3.3). It has 16 mm diameter double screw with 480 mm length, one feeding hopper and cooling unit with 1 l/min capacity. Because of one feeding hopper, sample (polymer and powders) must be pre-mixed and added to the extruder as such. By changing the exit head of the extruder, samples can be taken in round or flat strips. It can work minimum 100 g of sample.

Figure 3.3 ERNAM Gülnar brand twin screw extruder

Second extruder is the Buss (Switzerland) brand extruder in Hes Kablo R&D center (Figure 3.4).

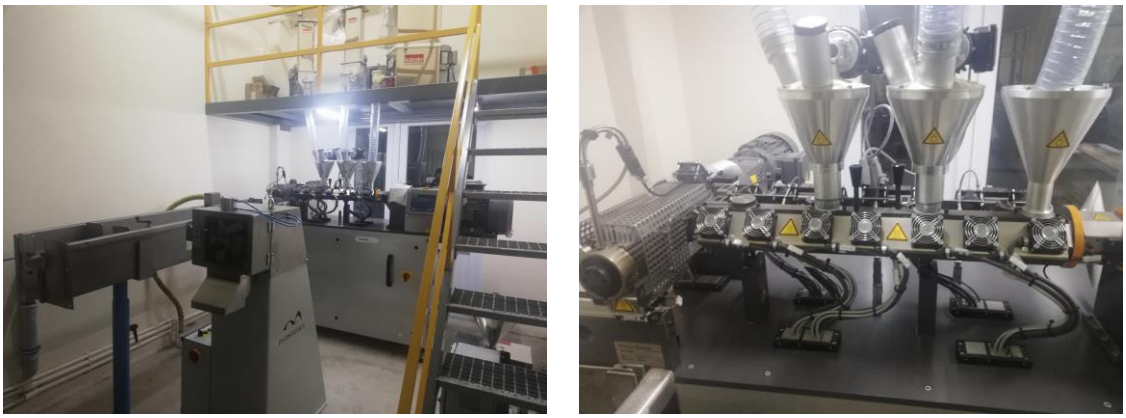

Figure 3.4 HES Kablo Buss brand single screw extruder

Buss MKS 30 extruder has 30 mm diameter single screw and 660 mm length and 3 gravimetric feeding hoppers. It is the laboratory model of original extruder that Hes Kablo using in production. There is no need to pre-mixing, because gravimetric scales are adding the polymer and powders with the percentage or weight that can be set before. It can work minimum 300 g of sample.

3.4 Comparison of the Flame Retardant Properties of $Al(OH)_3$ and $Mg(OH)_2$

$Al(OH)_3$ is used as the main filler material of halogen free flame retardant (HFFR) cables in Hes Kablo. To compare the flame retardant properties of $Al(OH)_3$ and $Mg(OH)_2$ and effect of grain size on flame retardancy, compound samples are prepared. These compounds are produced in extruder in ERNAM's polymer laboratory. As given in Table 3.1, three mixtures were prepared with $Al(OH)_3$ (1.5 μm grain size) , synthetic $Mg(OH)_2$ (1.5 μm grain size) and natural $Mg(OH)_2$ (brucite) (3 μm grain size) powders, provided that the polymer ratios were kept constant. Total 500 g of samples for each are mixed 30 minutes. The mixtures added to the extruder and temperature conditions are set as given Table 3.2.

Table 3.1 Polymer and filler ratios for compound production

Sample	Polymer	Filler		
	Concentration (%)	Concentration (%)		
	EVA (28% VA)	**$Al(OH)_3$**	**Synthetic $Mg(OH)_2$**	**Natural $Mg(OH)_2$**
1	100	-	-	-
2	70	30	-	-
3	70	-	30	-
4	70	-	-	30

Table 3.2 Operating conditions of extruder

Temperature (^oC)						Speed (rpm)	
Entrance	**Zone 1**	**Zone 2**	**Zone 3**	**Zone 4**	**Zone 5**	**Screw**	**Feeder**
35	160	170	170	160	150	200	10

The mould with 2.5 mm diameter hole on it was attached at the exit of extruder. The hot melt was cooled in 23 ^oC water bath and samples are cut with a length of 50 mm.

3.5 Preparation of Nano-sized $Mg(OH)_2$ Particles

3.5.1 Synthesis using $MgCl_2$ salt

For nano-sized particle synthesis, equation 3.1 was used.

$$MgCl_2.6H_2O + 2NH_3 \rightarrow Mg(OH)_2 + 2NH_4Cl + 6H_2O \quad \textbf{(3.1)}$$

The materials used in synthesis are given Table 3.3.

Table 3.3 Materials used for $Mg(OH)_2$ synthesis using $MgCl_2$ salt

Material	Quantity	Unit
$MgCl_2.6H_2O$	5,04	gram
H_2O	200	ml
NH_3	6	ml

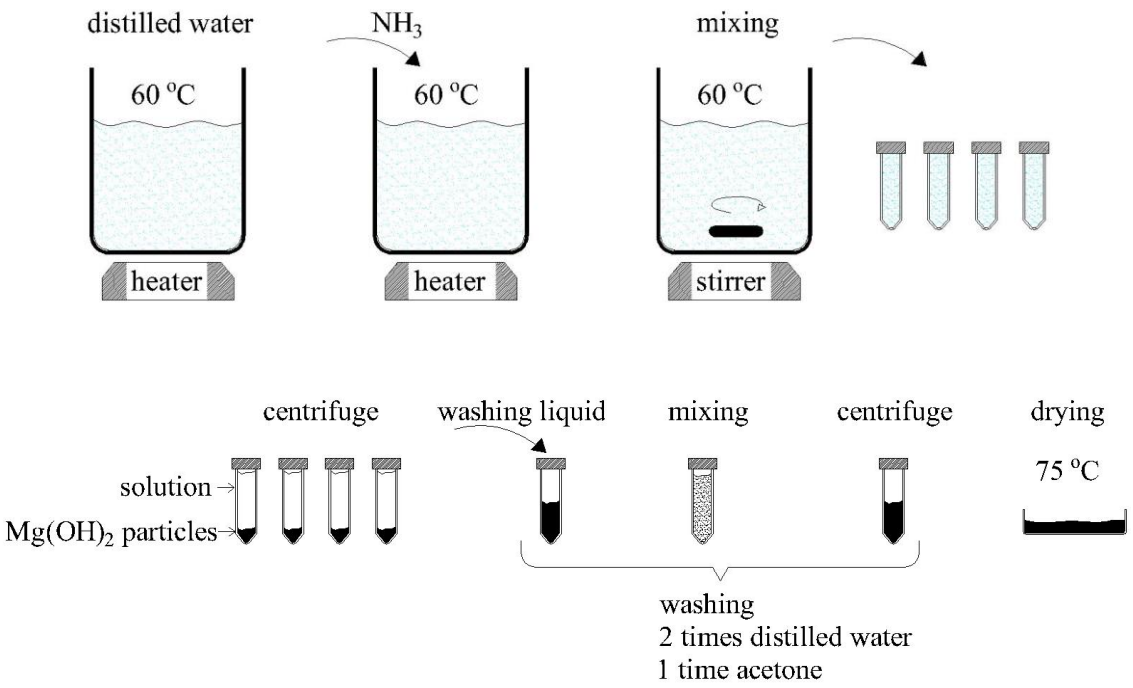

Figure 3.5 Schematic diagram for the preparation of $Mg(OH)_2$ nanoparticles

Schematic diagram for the preparation of $Mg(OH)_2$ nanoparticles is given in Figure 3.5. The distilled water is heated up to 60°C. At this temperature, $MgCl_2.6H_2O$ (Maltaş,Turkey) salt was added to the water and mixed 1 hour. 6 ml of NH_3 (25% Tekkim, Turkey) added to the solution in drops. The solution was mixed at 300 rpm using a magnetic stirrer for 24 hours to achieve homogenous mixtures. Solution was taken into 50 ml tubes and centrifuged at 4,000 rpm for 6 minutes. After removing the solution on the precipitated materials, the precipitates were taken into a single tube. Distilled water was again added to this tube and mixed. The mixture was again centrifuged at 4,000 rpm for 6 minutes. The water on the precipitate was removed, the same process was repeated 1 time by distilled water and 1 time by adding acetone. After the acetone on the precipitate was removed for the last time, the material was placed in the oven and dried for 5 hours at 75°C.

3.5.2 Synthesis using $Mg(NO_3)_2$ salt

Synthesis carried out according to equation 3.2

$$Mg(NO_3)_2.6H_2O + 2NH_3 \rightarrow Mg(OH)_2 + 2NH_4NO_3 + 4H_2O \quad \textbf{(3.2)}$$

The materials used in synthesis are given Table 3.4. The synthesis was carried out using the same steps as in the synthesis using magnesium chloride salt. Only magnesium nitrate (Maltaş,Turkey) was used as salt.

Table 3.4 Materials used for $Mg(OH)_2$ synthesis using $Mg(NO_3)_2$ salt

Material	Quantity	Unit
$Mg(NO_3)_2.6H_2O$	5.06	gram
H_2O	400	ml
NH_3	15	ml

3.5.3 Synthesis using $MgSO_4$ salt

Synthesis carried out according to equation 3.3

$$MgSO_4 + 2NH_3 + 4H_2O \rightarrow Mg(OH)_2 + 2NH_4SO_4 + 2H_2O \quad \textbf{(3.3)}$$

Table 3.5 Materials used for $Mg(OH)_2$ synthesis using $MgSO_4$ salt

Material	**Quantity**	**Unit**
$MgSO_4$	5,08	gram
H_2O	435	ml
NH_3	15	ml

The materials used in synthesis are given Table 3.5. The synthesis was carried out using the same steps as in the synthesis using magnesium nitrate salt. Only magnesium sulphate (Maltaş,Turkey) was used as salt.

3.6 Factory scale Production of Nano-sized $Mg(OH)_2$ Particles

200 L distilled water (conductivity 2-3 μS/cm) was put into the reactor and its temperature was raised to 60 °C. 4000 g $Mg(SO)_4$ was added to the water and mixed. 60 ml of HCl (37% Merck, Germany) was also added into the solution to decompose the impurities. The solution stirred into the reactor for 24 hours and filtered 6 times with paper filter which has 3-5 μm pore size. 3500 ml ammonia (Tekkim, Turkey) was added with 2.4 ml/min flow rate to the mixture of water and magnesium sulfate over 24 hours with the help of a tap beaker and continued mixing during this time. The solution was transferred to a separate container with a tap and left to rest another 24 hours for precipitation the magnesium hydroxide grains in it. The tap was mounted on the container at a point that remained above the precipitate level. Thus, the ammonium sulfate and water solution remaining in the upper part was removed through the tap. 100 l distilled water was added on precipitate for washing and mixed. After 16 hours, precipitation occurred and the remaining water on the top was drained from the tap. This process was repeated 3 times in total. After the last wash, the precipitate was placed in a large-bottomed container in an oven at 75°C and dried for 48 hours. Schematic diagram for the factory scale preparation of $Mg(OH)_2$ nanoparticles is given in Figure 3.6.

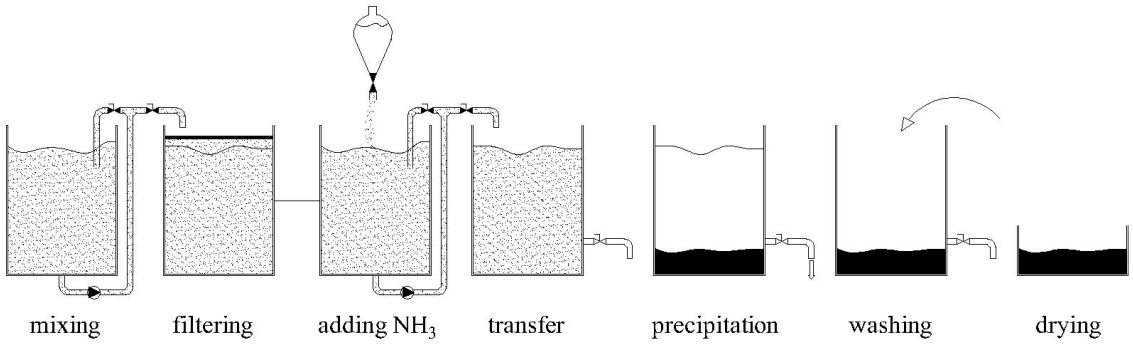

Figure 3.6 Schematic diagram for the factory scale preparation of $Mg(OH)_2$ nanoparticles

In Table 3.6, the materials used for synthesis and obtained powder quantity are given.

Table 3.6 Materials used for $Mg(OH)_2$ synthesis and obtained powder quantity

Synthesis number	$Mg(SO)_4$ (g)	Distilled water (l)	NH_3 (ml)	HCl (ml)	Synthesized $Mg(OH)_2$ (g)
1	4,000	210	3,500	60	432
2	4,000	210	3,500	60	395
3	4,000	210	3,000	50	418
4	4,000	210	3,500	60	453
5	4,000	210	3,500	60	460
6	4,000	210	3,500	60	450
7	4,000	210	3,500	60	420
8	4,000	210	3,500	60	425

3.7 Compound Production

For compound production, Buss MKS 30 extruder in Hes Kablo R&D center was used.

Table 3.7 Produced compounds and their contents

Compound	Ethylene Vinyl Acetate (EVA) (%)	$Al(OH)_3$ (%)	$Mg(OH)_2$ (synthetic) (%)	$Mg(OH)_2$ (nano-sized) (%)
1	100	-	-	-
2	40	60	-	-
3	40	-	60	-
4	40	59	-	1
5	40	57	-	3
6	40	55	-	5
7	40	51	-	9
8	40	50	-	10
9	40	-	59	1
10	40	-	57	3
11	40	-	55	5
12	40	-	51	9
13	40	-	50	10
14	40	-	48	12

Table 3.8 Operating conditions of Buss MKS 30 extruder

Temperature (ºC)						Speed (rpm)
Entrance	**Zone 1**	**Zone 2**	**Zone 3**	**Zone 4**	**Zone 5**	**Screw**
50	120	130	150	180	190	287

There are scales under the hoppers of MKS 30 that also show the weight of the material inside. In this way, a formula can be created by entering only the mixture percentages or the material weights to be mixed. The "%" rates for the produced compound samples were entered as specified in Table 3.7. Since there were 2 powder hoppers in the extruder, the hoppers were completely emptied and cleaned, before new powders were loaded. Also, before the production of each compound sample, only EVA polymer was given to the extruder for 3 minutes, so that the dust residues inside were cleaned. Operating conditions of extruder is given in Table 3.8. The extruder exit head mould was produced for the production of strip material with a diameter of only 3 mm. However, as a flat sample was required in the experiments, a new mould was designed and manufactured to take a flat sample of 15 mm width and 3 mm thickness. The hot material coming out of the extruder was cooled by passing through a 2 m long cooling pool containing water at 25ºC. The cooled compound was pulled at a speed of 3 m/min through a caterpillar, allowing sample production in equal dimensions. For each compound formula, 30 cm length 10 samples were taken.

3.8 Characterization

3.8.1 Determination of Flame Retardant Property

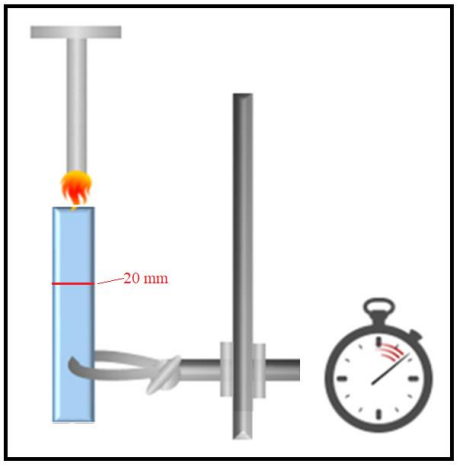

Figure 3.7 Burning time measuring test set-up

The extruded 50 mm length and 2.5 mm diameter samples in ERNAM's laboratory were marked from their 20 mm length. They were ignited from above with flame source with a flame height of 16 mm and the time is measured until the 20 mm length burned as given in Figure 3.7.

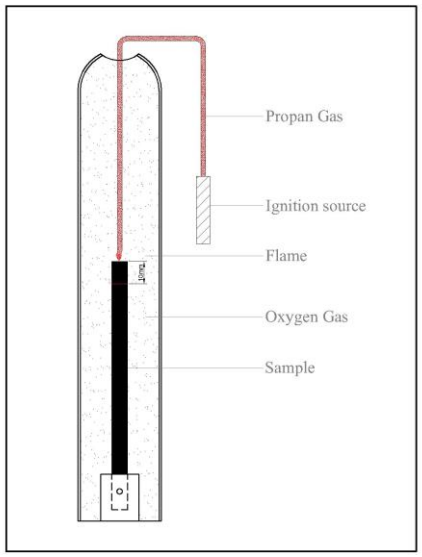

Figure 3.8 Oxygen atmosphere vertical burning test set-up

The extruded samples in Hes Kablo are prepared with size of 110 mm x 7 mm and 2.5 mm thickness. They marked from their 10 mm length. Since the samples had flame retardant additives, the test was carried out in an environment with an oxygen ratio of 43.7% in order to ensure combustion up to the marked area. They were ignited from above with flame source with a flame height of 16 mm and the time is measured until 10 mm length burned. The oxygen atmosphere vertical burning set-up is given in figure 3.8.

3.8.2 SEM Analysis

Scanning electron microscope (ZEISS LS-10 Life Science) in ERNAM was used to analyze grain structure of lab-scale synthesized magnesium hydroxide powders at 25 kV. SEM images were taken between 20,000 and 50,000 magnifications.

Scanning electron microscope (ZEISS Gemini) in AGU was used to analyze grain structure of factory-scale synthesized magnesium hydroxide and commercial synthetic magnesium hydroxide powders at 1 kV. SEM images were taken between 1,000 and 57,000 magnifications. The samples were coated with gold before the analysis. The sizes of particles were also measured. Energy dispersive X-ray spectroscopy (EDX) analysis obtained during SEM analysis.

3.8.3 Fourier-Transform Infrared Spectroscopy (FT-IR) Analysis

FT-IR measurement was conducted to determine the functional groups in synthesized magnesium hydroxide powders. The measurement was carried out with an Agilent (Cary 630) device between 400-4,000 cm-1 wavelength (between the visible and microwave wavelength range). The graphs of absorbance vs wavelength (nm) were plotted. 32 scans were performed for each spectrum.

3.8.4 X-ray Diffraction (XRD) Analysis

The purity of the samples was characterized by powder X-ray diffraction (XRD) using a Bruker D8Discover diffractometer. 2θ range was from 15-120^{o} and wavelength was used Cu Kα=0.15406 nm. Operation voltage was 40kV and current intensity was 30mA.

3.8.5 X-Ray Fluorescence (XRF) Analysis

The X-ray fluorescence analyses were performed on a Spectro Xepos spectrometer. When preparing samples for analysis, pressed pellets techniques were used. 5 g of sample and 1 g CEREOX BM-0002-1 wax were mixed for 5 minutes. The mixture was placed in a 32 cm diameter ring in press mold, pressed with a 15-ton weight. The sample, which was kept under pressure for 1 minute, was then removed from the ring and placed in the device.

3.8.6 Thermogravimetric (TGA) Analysis

Thermogravimetric analysis was carried out with a Shimadzu DTG-60H TG/DTA simultaneous measuring instrument. Temperature was selected 450 ^{o}C with a temperature rate 2 ^{o}C/min. Sample weights were 36.187 mg for commercial product and 16.731 g for synthesized product. The applying atmosphere was air.

3.8.7 Limiting Oxygen Index (LOI) Analysis

For determining the limiting oxygen index, a Fire Testing Technology Oxygen Index unit is used as shown in Figure 3.9.

Figure 3.9 Limiting oxygen index unit in Hes Kablo

Oxygen pressure in the device was set to be 2 bar and nitrogen pressure to be 2.5 bar. Samples of 110 mmx7mmx2.5 mm were prepared. The 5 mm parts, from the upper part of the samples, were marked. The samples, which were attached to the unit vertically by means of the fastener, were ignited by a propane gas igniter with a flame height of 16 mm.

3.8.7.1 Determination of Preliminary Oxygen Content

In the first part of the analysis, the preliminary oxygen concentration was determined. Here, the value limit where the combustion takes place was determined by increasing the oxygen rate. It was coded as (X) when combustion occurred and (O) when extinction occurred. For the combustion to be considered as taking place, the marked 5 mm of the sample must be burned within 180 seconds. In the range where the difference between the "X" and "O" values is <= 1% and the O-X sequence occurred, the value O was determined as the pre-oxygen concentration. (See Table 3.9 for example)

Table 3.9 Determination of preliminary oxygen content

Oxygen concentration (%)	25.0	30.0	35.0	32.0	33.0		
Burning Period (s)	20	130	<180	160	>180		
Length burnt (mm)	1	2,5	5	3	5		
Response (X or O)	O	O	X	O	X		

Preliminary oxygen concentration is (%) =32.0

3.8.7.2 Determination of the Oxygen Index Value

In this part of the analysis, the oxygen index based on the preliminary concentration was determined. Another sample was tested at preliminary concentration and its response was recorded. This test was recorded in the table as the first test belonging to the test series specified as N_L and N_T in the standard. A new sample with an oxygen concentration step size d = 0.2% was tested and its response was recorded. The test was repeated until a different response was observed in the first test. After the first value in which combustion was observed, the N_L series occurred. After a different response was recorded, four more samples were further tested to d = 0.2%. The tests in the N_L series and the last 5 tests constitute the N_T series. (See Table 3.10 for an example)

Table 3.10 Determination of the oxygen index value

N_T series measurements											
NL series measurements							c_F				
Oxygen concentration (%)	32.0	32.2	32.4	32.6			32.6	32.4	32.6	32.8	33.0
Burning Period (s)	150	160	160	>180			>180	155	160	165	>180
Length burnt (mm)											
Response (X or O)	O	O	O	→	→	→	X	O	O	O	X

Oxygen Index values are calculated according to Eq.3.4;

$$OI = c_F + k.d \tag{3.4}$$

c_F is final value of oxygen concentration used in N_T measurement series, *k* is coefficient taken from Table 3.11, d is interval expressed in volumetric fraction percentage.

Table 3.11 Values of k for calculating oxygen index concentration

1	2	3	4	5	6
Responses for the last five measurements	(a) O	OO	OOO	OOOO	
XOOOO	-0.55	-0.55	-0.55	-0.55	OXXXX
XOOOX	-1.25	-1.25	-1.25	-1.25	OXXXO
XOOXO	0.37	0.38	0.38	0.38	OXXOX
XOOXX	-0.17	-0.14	-0.14	-0.14	OXXOO
XOXOO	0.02	0.04	0.04	0.04	OXOXX
XOXOX	-0.50	-0.46	-0.45	-0.45	OXOXO
XOXXO	1.17	1.24	1.25	1.25	OXOOX
XOXXX	0.61	0.73	0.76	0.76	OXOOO
XXOOO	-0.30	-0.27	-0.26	-0.26	OOXXX
XXOOX	-0.83	-0.76	-0.75	-0.75	OOXXO
XXOXO	0.83	0.94	0.95	0.95	OOXOX
XXOXX	0.30	0.46	0.50	0.50	OOXOO
XXXOO	0.50	0.65	0.68	0.68	OOOXX
XXXOX	-0.04	0.19	0.24	0.25	OOOXO
XXXXO	1.60	1.92	2.00	2.01	OOOOX
XXXXX	0.89	1.33	1.47	1.50	OOOOO
	Values of *k* for which the first NL determinations are: (b) X XX XXX XXXX are as given in the above table opposite the appropriate response in column 6, but with the sign of *k* reversed.				Responses for the last five measurements

3.8.7.3 Verification of the Oxygen Concentration Increment

Last six results	Oxygen concentration (%)			
	c_i	OI	c_i-OI	$(c_i\text{-}OI)^2$
c_F 1				
2				
3				
4				
5				
n 6				
	Total $\Sigma(c_i\text{-}OI)^2$			

Standard deviation is calculated according to Eq. 3.5 ;

$$\hat{\sigma} = \left[\frac{\Sigma(c_i - OI)^2}{n-1}\right]^{1/2} \quad \textbf{(3.5)}$$

If $\frac{2\hat{\sigma}}{3} < d < \frac{3\hat{\sigma}}{2}$ or if $d > \frac{3\hat{\sigma}}{2}$ and d=0.2 % then OI is valid.

For each sample, LOI values were found, and these values has been verified by calculating standard deviation.

3.8.8 Elongation and Tensile Strength Tests

Elongation and tensile tests were performed in Hes Kablo on a Zwick/Roell Z030 (Figure 3.10) with a capacity of 2.5 kN. % elongation and tensile strength values were automatically calculated by Zwick/Roell software and recorded. Tests were carried out with a speed of 250 mm/min. Test specimens' length were 250 mm and with a thickness of 2.5 mm.

Figure 3.10 Zwick/Roell tensile test device in Hes Kablo

Chapter 4

4. Result and Discussion

4.1 Comparison of Flame Retardant Property of Materials

In this experiment, samples were produced by mixing magnesium hydroxide (MDH), which is produced by the synthesis method, magnesium hydroxide (Brucite), which is a mineral in nature, and aluminum hydroxide (ATH) used in Hes Kablo's formulas with ethylene vinyl acetate (EVA) copolymer in the same proportions. The results obtained as a result of the burning tests are given in Figure 4.1.

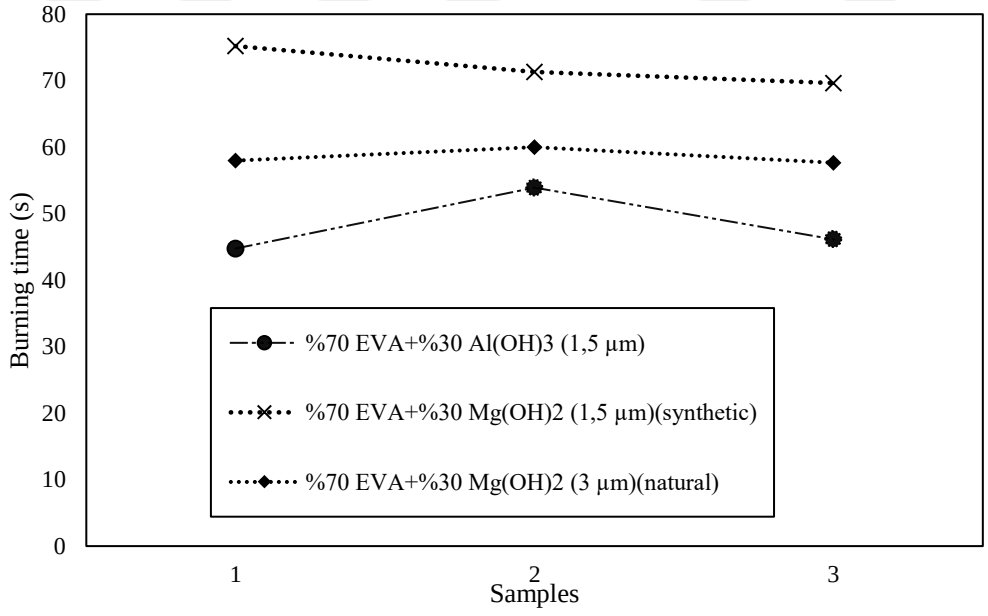

Figure 4.1 Burning times of 2.5 mm diameter, 2 cm length compound samples

Natural magnesium hydroxide is a mineral found in nature and is brought into powder form by grinding. The grain size that can be reached with this method is limited. The smallest grain size available in the market is around 3 micrometers.

Synthetic magnesium hydroxide used in this study is produced from the mineral serpentinite ($Mg_3Si_2O_5(OH)_4$). First magnesium oxide is produced from the serpentinite mineral, and then magnesium hydroxide is produced from magnesium oxide [45]. With this method, higher purity and much smaller grain sizes can be achieved.

As a result of this experiment, it was seen that the synthetic magnesium hydroxide with 1.5 µm grain size showed the best combustion performance. Although natural magnesium hydroxide outperformed aluminum hydroxide, it did not reach the values of synthetic product. In addition to the larger grain sizes of natural magnesium hydroxide, its impurity also influences getting these results. In Figure 4.2, the sharp and intense peak at 3695 cm^{-1} is the -OH group in $Mg(OH)_2$. Synthetic $Mg(OH)_2$ also appears to have a sharper peak, while natural $Mg(OH)_2$ also has a lower absorbance value. In addition, impurities in natural $Mg(OH)_2$ at wavelengths of 900 cm^{-1}, 100 cm^{-1} and 1430 cm^{-1} were clearly observed.

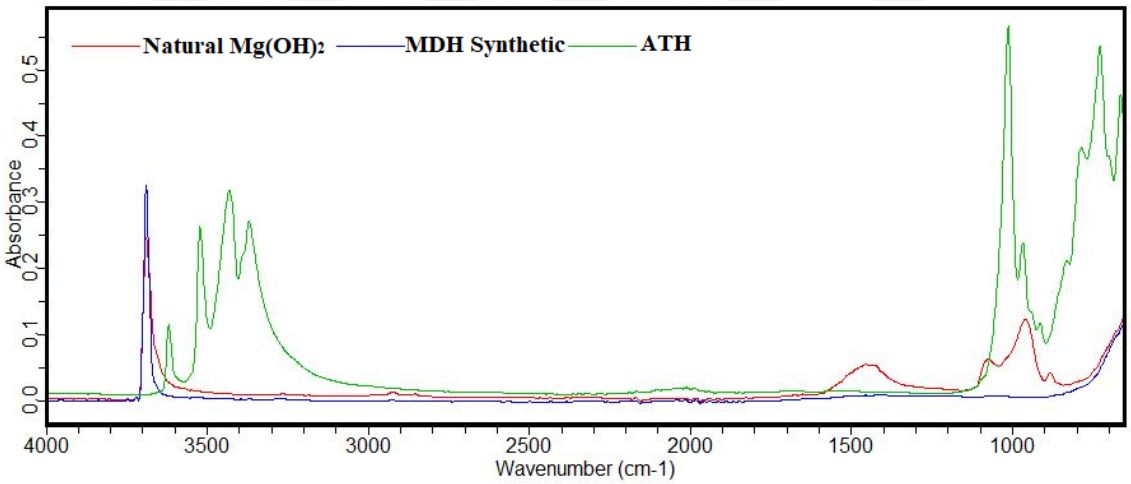

Figure 4.2 FT-IR results of natural $Mg(OH)_2$ (3 µm grain size), synthetic $Mg(OH)_2$ (1.5 µm grain size), ATH (1.5 µm grain size)

4.2 Comparison of Nano-sized Particles Synthesized from Different Salts

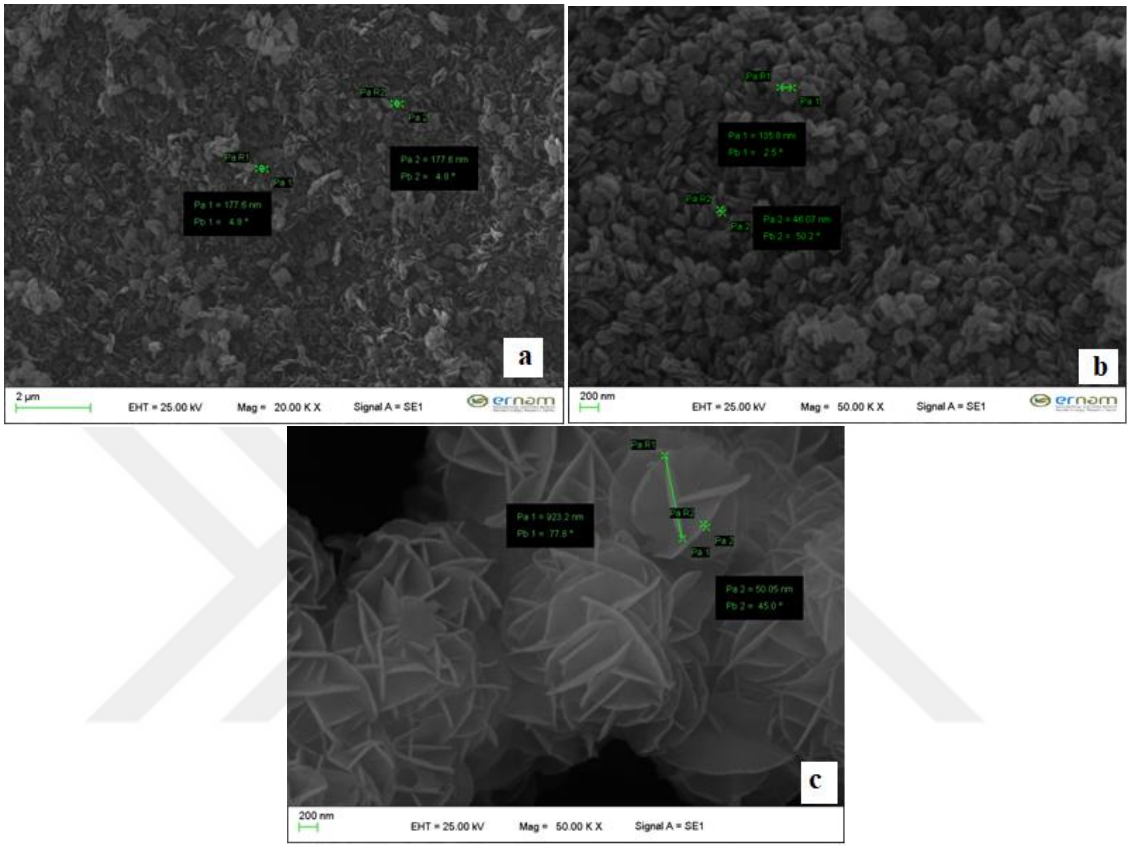

Figure 4.3 SEM images of synthesized nano-sized $Mg(OH)_2$ particles. (a) Synthesized from $MgCl_2$, (b) Synthesized from $Mg(NO_3)_2$, (c) Synthesized from $Mg(SO_4)$

SEM images of synthesized $Mg(OH)_2$ particles from $MgCl_2$, $Mg(NO_3)_2$ and $Mg(SO_4)$ salts are given in Figure 4.3. As can be seen from the figure, particles synthesized from magnesium chloride salt consist of fine and long grains. Although the grain sizes are relatively variable between 150-200 nm, the distribution of the grains is not very regular. It was observed that the particle structures of the particles synthesized from magnesium nitrate salt were formed in round form. The grain sizes are fairly equal and their distribution is fairly uniform. It was seen that the grain sizes formed between 50-100 nm diameter and grain sizes were smaller than other salts. The particles synthesized from magnesium sulfate were in the form of thin plates with very large

surface areas with a thickness of 5-10 nm and lengths reaching 900 nm in places. The particles were mostly seen in the form of nanoflowers.

Table 4.1 Comparison of salt prices

Salt (Pure)	**$MgCl_2$**	**$Mg(NO_3)_2$**	**$MgSO_4$**
Molecular weight	95.21	148.33	120.38
The weight of Mg in 1 kg (g)	255.33	163.89	201.94
Price (USD/kg)	4.3	5.5	2.3
Price of Mg weight in 1 kg (USD)	0.016	0.033	0.011

Since the magnesium hydroxide to be synthesized will be used commercially, the cost of the salt to be used in the synthesis is also important. Therefore, as can be seen in Table 4.1, price comparisons were made according to the Mg content of the salts. It was seen that $MgSO_4$ in three salts was more advantageous in terms of cost.

Table 4.2 Obtained by-products according to the salts used.

Chemical Equation	**By Product**
$MgCl_2 + 2NH_3 \rightarrow Mg(OH)_2 + 2NH_4Cl$	Ammonium Chloride
$Mg(NO_3)_2 + 2NH_3 + H_2O \rightarrow Mg(OH)_2 + 2NH_4NO_3$	Ammonium Nitrate
$MgSO_4 + 2NH_3 + 4H_2O \rightarrow Mg(OH)_2 + 2NH_4SO_4 + 2H_2O$	Ammonium Sulphate

The second point of attention here was the by-products obtained as a result of synthesis (Table 4.2). Ammonium nitrate, despite the use of fertilizers in agriculture, because it is used in the production of hand-made explosives was banned in Turkey. Ammonium chloride is used in many areas from the cosmetic industry to the leather industry, from the pharmaceutical industry to the metal industry. Ammonium sulphate is one of the most used agricultural fertilizers in the market. When these results were evaluated, it was deemed appropriate to use Magnesium sulphate as the synthesis salt.

4.3 Comparison of Commercial $Mg(OH)_2$ and Factory-scale Synthesized $Mg(OH)_2$ Nanoparticles

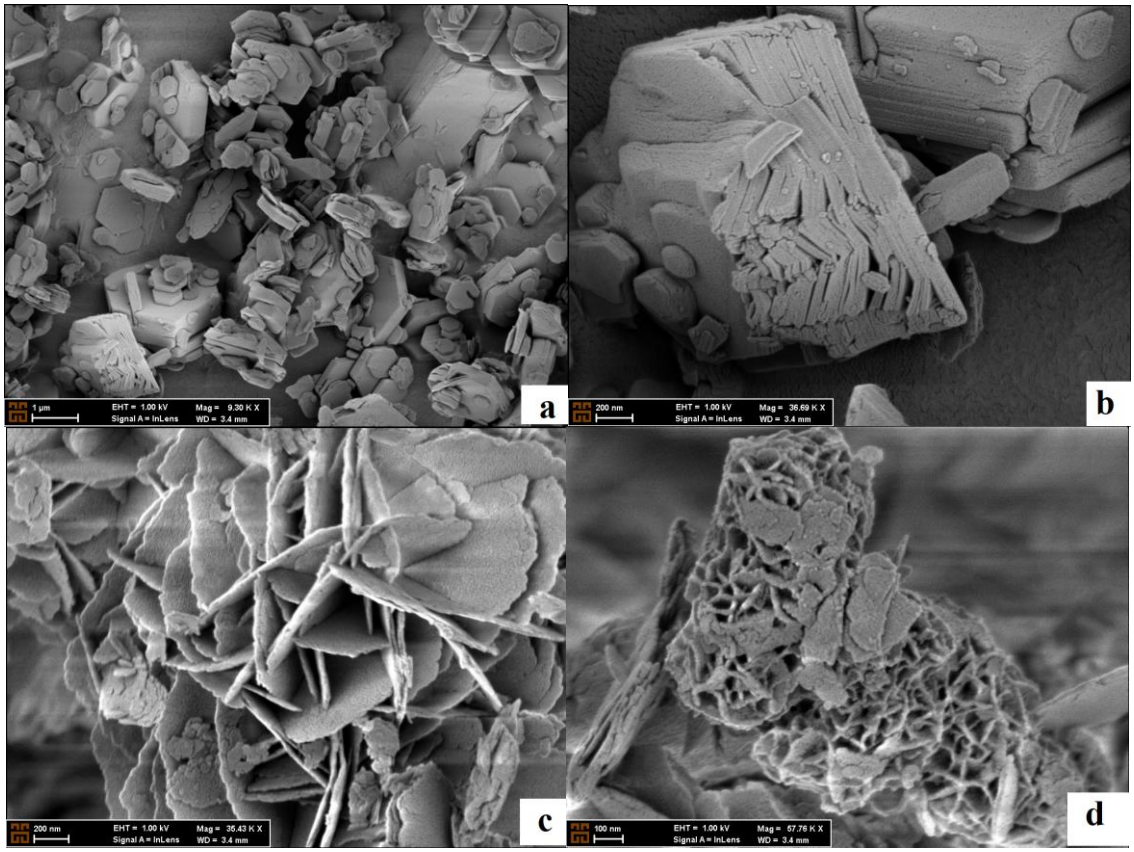

Figure 4.4 SEM images (a) and (b) Commercial $Mg(OH)_2$ particles (c) and (d) Factory-scale synthesized $Mg(OH)_2$ nano-particles

Commercial $Mg(OH)_2$ is produced from serpentine mineral by means of a hydrochloric acid recycle process. $MgCl_2$ is produced after leaching of serpentine with hydrochloric acid. After thermally decomposing of $MgCl_2$ brine, MgO powders are formed. In a hydration process, magnesium oxide particles are converted $Mg(OH)_2$. [35] As can be seen on Figure 4.4 (a) and (b) SEM images, multi-layered hexagonal particles were formed. The distances on the surfaces of these agglomerated particles range from 500 nm to 1 μm. Factory-scaled particles consist of plates with a thickness of 5-10 nm and the widest distance on their surface varying between 50 nm and 1 μm. Since these nanoplates do not agglomerate homogeneously, a much larger surface area was created than the commercial product.

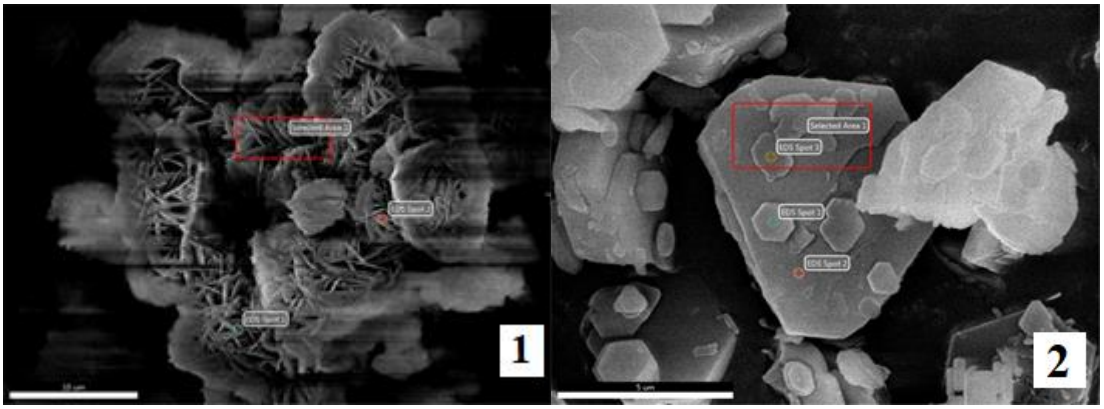

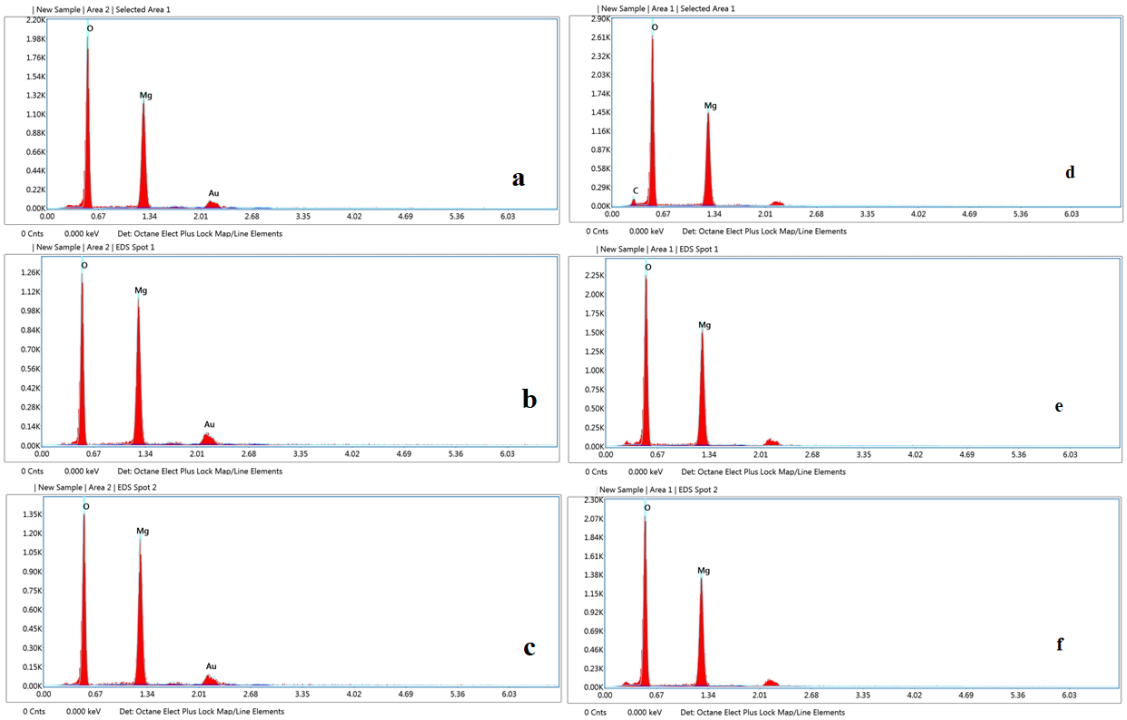

Figure 4.5 EDX Analysis (1),(a),(b) and (c) factory-scale nano particles (2),(d),(e) and (f) commercial product

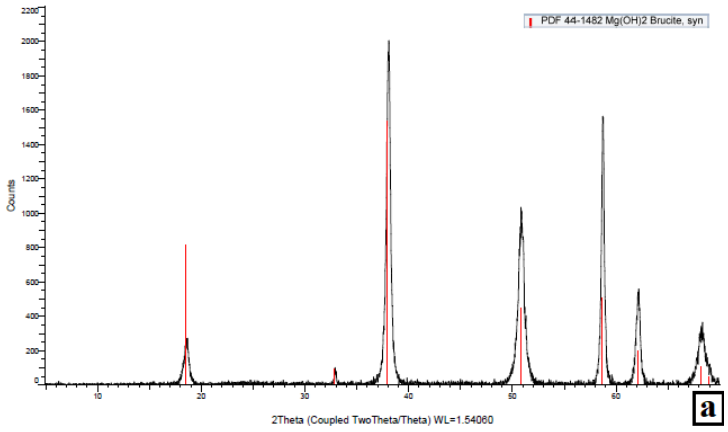

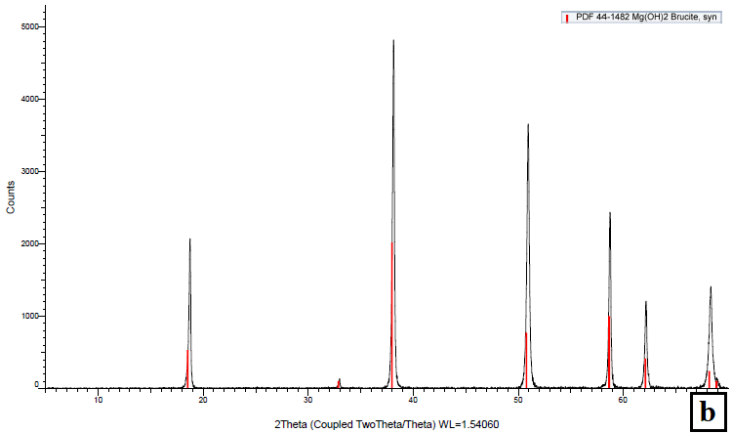

Figure 4.6 XRD Results of (a) Factory-scale synthesized nano particles (b) commercial product

As can be seen in Figures 4.5 and 4.6, EDX and XRD analysis performed on the factory scale synthesized nano particles and commercial $Mg(OH)_2$ product showed that both product has high quality.

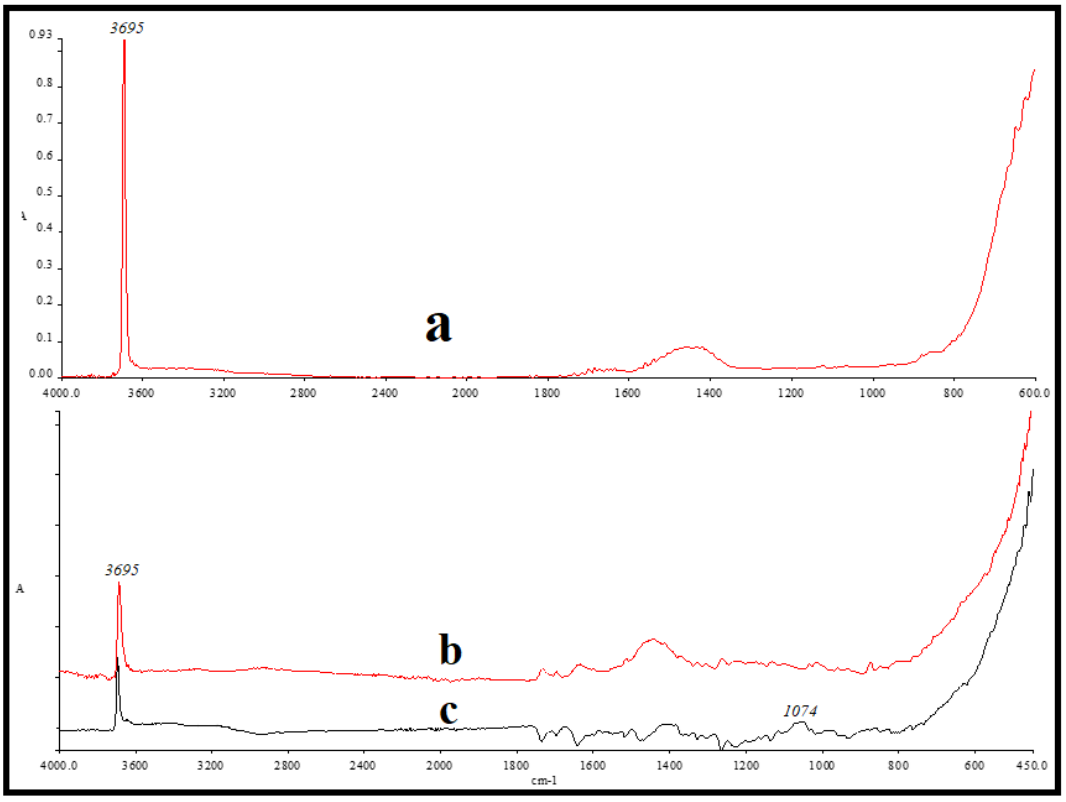

Figure 4.7 FT-IR Results of (a) Magnesium hydroxide (b) commercial product (c) Factory-scale synthesized nano particles

FT-IR spectrum results are shown in Figure 4.7. The peak at 3695 cm^{-1} is due to the OH groups and can be seen in spectrum of both samples. The band at 1074 cm^{-1} is spectrum of synthesized product represents the stretching of Si-O.

Table 4.3 XRF Results of commercial and synthesized products

Element		Concentration (%)	
Formula	**Name**	**Commercial Product**	**Synthesized Product**
MgO	Magnesium oxide	61.36	57.78
Al_2O_3	Aluminum oxide	0.0120	0.0313
CaO	Calcium oxide	0.0176	0.146
SiO_2	Silicon dioxide	0.0576	0.3435
Fe_2O_3	Iron (III) oxide	0.0155	0.3721
SO3	Sulfur trioxide	-	2.723

Table 4.3 XRF analysis results are showed that, the commercial product is purer than synthesized product. This is directly proportional to the purity of the Magnesium sulphate mineral from which the nanoparticles are synthesized. Much purer nanoparticles can be obtained by using purer salt.

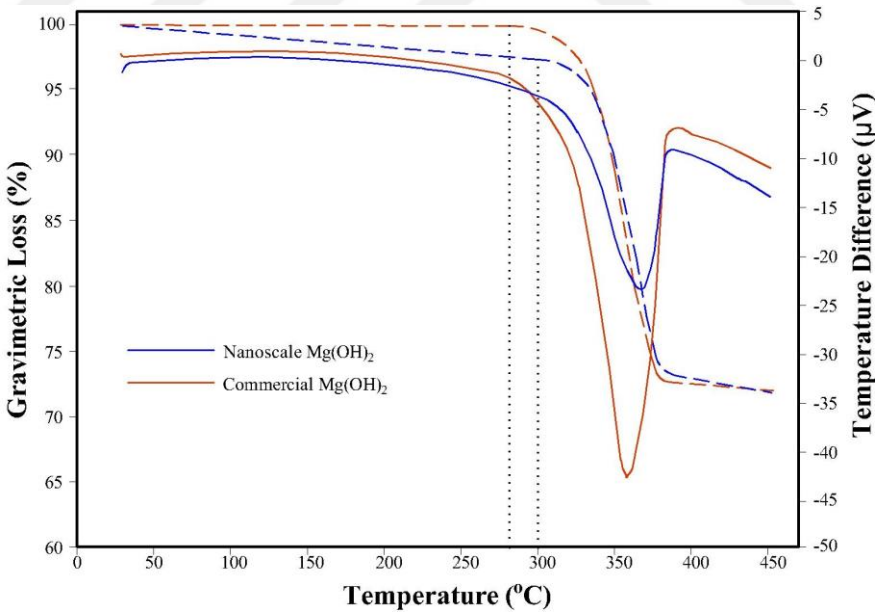

Figure 4.8 TG and DTA curves of synthesized and commercial products

The thermal degradation test of factory-scale synthesized nano product and commercial product samples are studied the weight loss and temperature difference showed in Figure 4.8. Approximately 3% of weight loss is found in the range of 100-300°C. This showed that despite drying, there was still a small amount of moisture in the

synthesized product. This 3% weight loss is due to the evaporation of moisture in the product. Major weight loss is started around 300^{o}C due to decomposition of magnesium hydroxide.

The commercial product showed no weight loss between 0-280°C. This indicates that there is no moisture residue in the product. Thermal decomposition started around 280^{o}C.

When these results were compared, it was seen that the thermal decomposition temperature of the product synthesized at nano scale was higher than the commercial product.

4.4 Comparison of Flame Retardant Property of Compounds

4.4.1 FT-IR Analysis of Compounds

In Figure 4.9 FT-IR spectra of polyethylene and EVA polymers are given to show the peaks which are due to PE and EVA in FT-IR spectra of compounds. In Figure 4.10 the peaks at 3695 cm^{-1} show the nano-sized $Mg(OH)_2$ particles in the compounds. The large band around 3400 cm^{-1} is due to -OH groups in ATH.

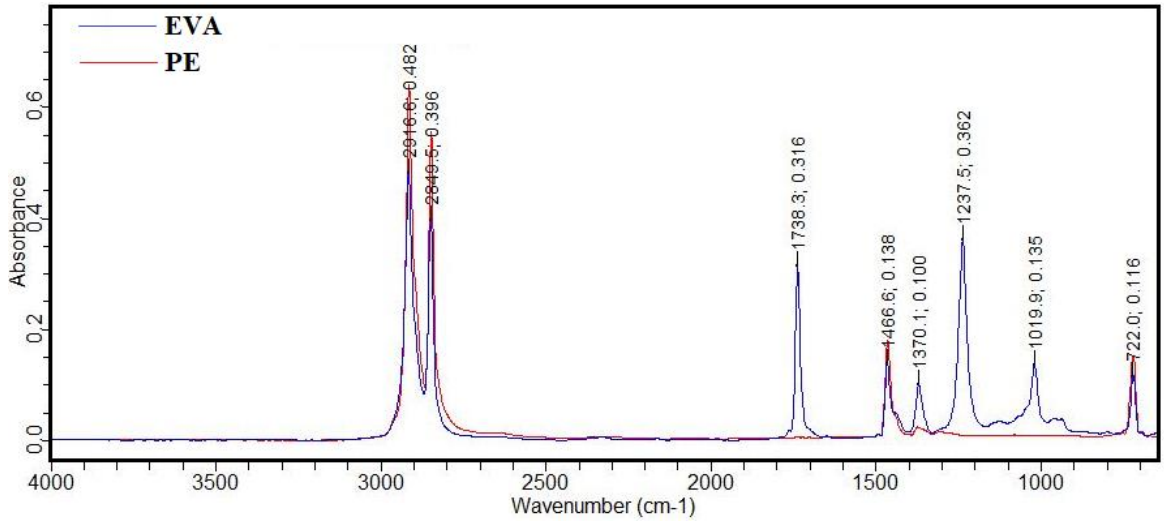

Figure 4.9 FT-IR spectra of Polyethylene and Ethylene vinyl acetate

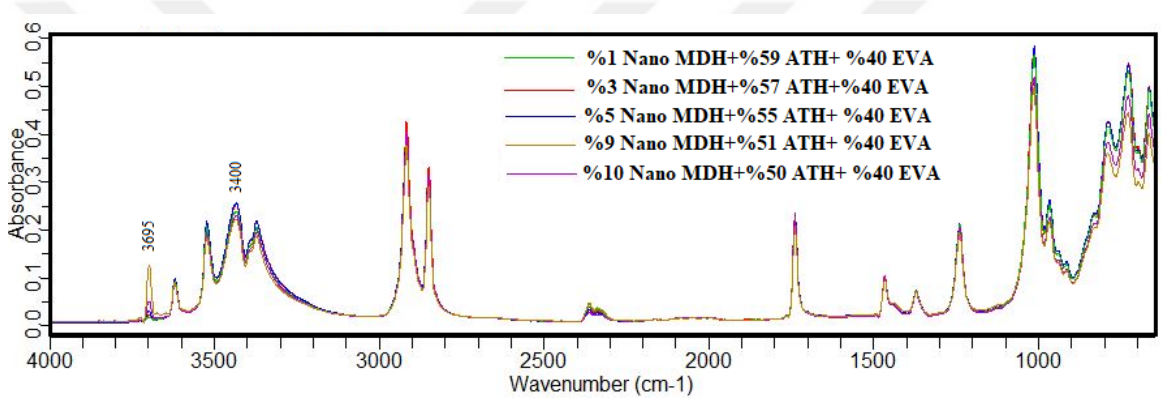

Figure 4.10 FT-IR spectra of compound samples prepared with 1-3-5-9-10% nano-sized $Mg(OH)_2$ and ATH

As given in Figure 4.11, with the addition of nano-sized $Mg(OH)_2$ particles total rate of magnesium hydroxide reached 60% in total; and the peaks due to -OH groups in $Mg(OH)_2$ was seen sharply and intensely at 3695 cm^{-1}.

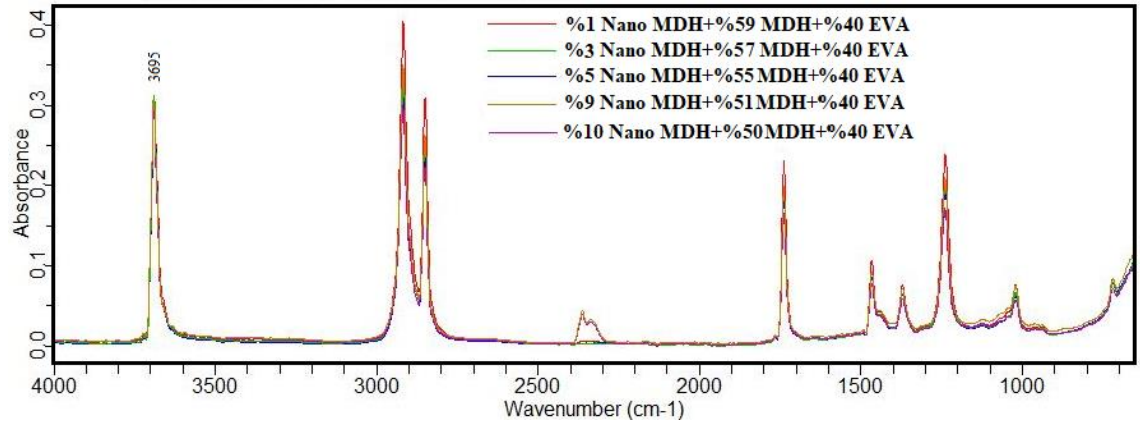

Figure 4.11 FT-IR spectra of compound samples prepared with 1-3-5-9-10% nano-sized $Mg(OH)_2$ and MDH

4.4.2 Limiting Oxygen Index Values

As an example, LOI calculation of 1% nano MDH added ATH (Eti) and MDH (Magnifin) samples are given in Table 4.4 and Table 4.5.

Table 4.4 Determination of preliminary oxygen content of 1% Nano MDH+ATH

Oxygen concentration (%)	28.0	29.0	30.0				
Burning Period (s)	100	110	<180				
Length burnt (mm)	3	3.5	5				
Response (X or O)	O	O	X				

Preliminary oxygen concentration is (%) =29.0

Table 4.5 Determination of the oxygen index value of 1% Nano MDH+ATH

N_T series measurements											
NL series measurements							c_F				
Oxygen concentration (%)	29.0	29.2					29.2	29.0	29.2	29.4	29.2
Burning Period (s)	110	>180					>180	100	120	>180	>180
Length burnt (mm)											
Response (X or O)	O		→				X	O	O	X	X

From Table 3.10, N_L is "O" and response of last five measurements "XOOXX", then *k* value is found "-0.17". d=0,2, c_F is last result =29.2

From Eq. 3.1;

$$\boldsymbol{OI} = c_F + k.d = 29{,}2 + (-0{,}17x\ 0{,}2) = \mathbf{29,16}$$

Limiting Oxygen Index value of 1% Nano MDH+59% ATH+40% EVA is **29.16.**

Table 4.6 Verification of the oxygen concentration increment

Last six results		Oxygen concentration (%)			
		c_i	OI	c_i-OI	$(c_i\text{-}OI)^2$
c_F	1	29.2	29.16	0.04	0.0016
	2	29.4	29.16	0.24	0.0576
	3	29.2	29.16	0.04	0.0016
	4	29.0	29.16	-0.16	0.0256
	5	29.2	29.16	0.04	0.0016
n	6	29.0	29.16	-0.16	0.0256
		Total $\Sigma(c_i\text{-}OI)^2=0.1136$			

$$\hat{\sigma} = \left[\frac{\Sigma(c_i - OI)^2}{n-1}\right]^{1/2} = \left[\frac{0{,}1136}{6-1}\right]^{1/2} = \mathbf{0.15}$$

$\frac{2\hat{\sigma}}{3} = 0{,}1 \quad \frac{3\hat{\sigma}}{2} = 0.225 \qquad 0{,}1 < 0.2 < 0.225$ with these results OI value is valid.

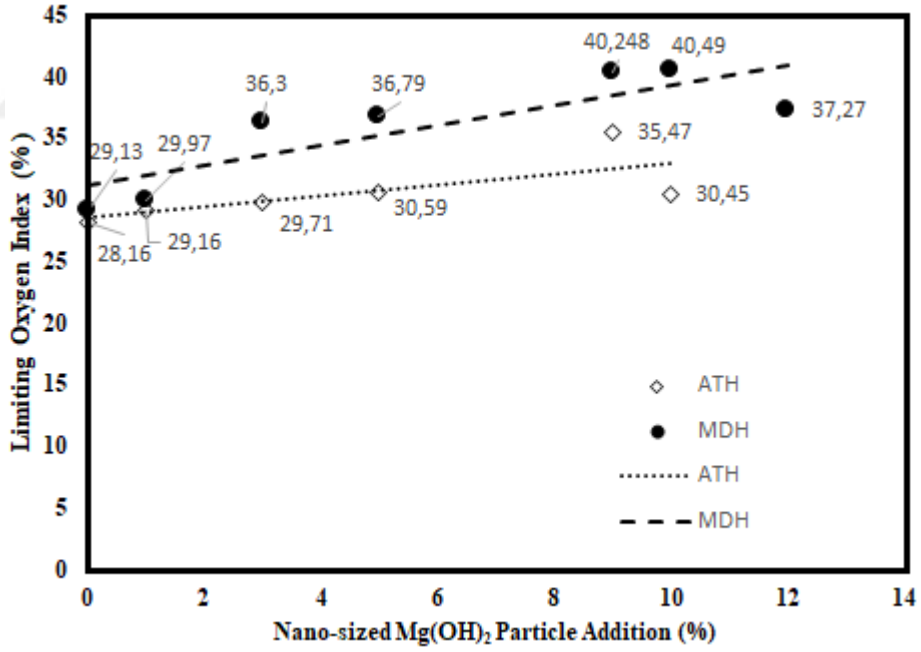

Figure 4.12 Nano-sized $Mg(OH)_2$ particles additive dependent limiting oxygen index values

As can be seen from Figure 4.12, it was observed that addition of nano-sized $Mg(OH)_2$ was contributed the increasing of the LOI values both with ATH and MDH compound samples. As the percentage of the nano-sized $Mg(OH)_2$ particles added in the

compound increased, the LOI values of compounds also increased. However, when more than 9% nano-sized $Mg(OH)_2$ was added to the compound containing ATH, it was observed that the LOI value decreased. The same situation occurred when the MDH-containing samples exceeded 10% additive level. The compound sample prepared using 100% nano-sized $Mg(OH)_2$ powder (60% nano-sized $Mg(OH)_2$+60% EVA), LOI value is found 23%.

4.4.3 Vertical Burning Test Results

Vertical burning tests were carried out by measuring the burning time of the 5 mm upper part of the samples.

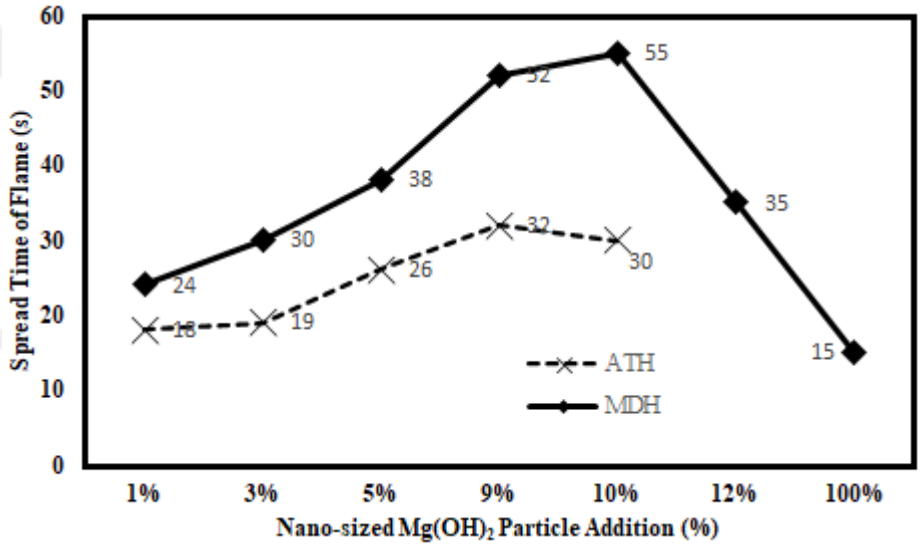

Figure 4.13 Nano-sized $Mg(OH)_2$ particles additive dependent vertical burning results

In Figure 4.13, vertical burning test results of compounds depending on nano-sized $Mg(OH)_2$ addition is given. It was observed that the burning test results were parallel with the LOI test results. As the nano-sized $Mg(OH)_2$ particle addition increased, the spreading time of flame was also increased. However, as can be seen again from Figure 4.13, it was observed that when the nano-sized $Mg(OH)_2$ particle additive exceeded 9% in ATH-containing compound samples and 10% in compound samples containing MDH, there was an increase in the spread time of the flame. In the compound sample made using 100% nano-sized $Mg(OH)_2$ powder (60% nano-sized $Mg(OH)_2$+60% EVA), the burning time reduced to 15 seconds.

4.4.4 Elongation and Tensile Strength Tests

In Figure 4.14, elongation test results of compounds are given. As can be seen from figure, elongation values were decreased with the increase of addition of nano-sized $Mg(OH)_2$ to both ATH and MDH based samples. It was observed that the elongation values increased again after 9% nano product addition in ATH based samples and after 10% nano product addition in MDH based samples.

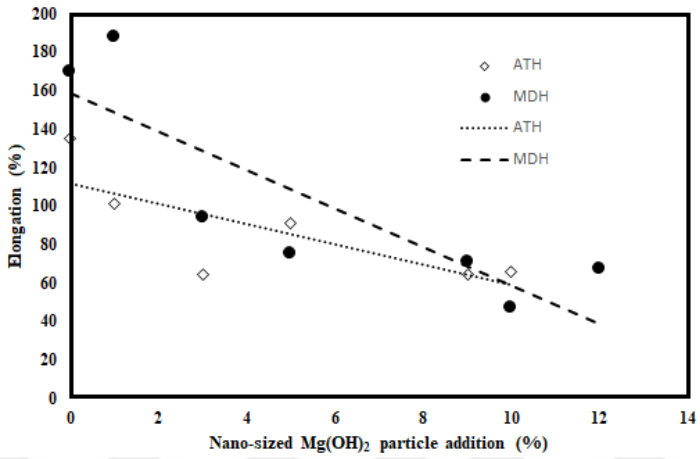

Figure 4.14 Nano-sized $Mg(OH)_2$ particles additive dependent change of elongation values

It was observed that tensile strength values also changed inversely depending on the elongation values. As can be seen in Figure 4.15, the tensile strength values were 966 N/mm^2 in nano-sized $Mg(OH)_2$ additive-free ATH based samples, and when the nano product additive level was 9%, it increased to 1100 N/mm^2. It was also observed that when there was no nanoparticle additive in MDH-based samples, the tensile strength value was 1468 N/mm^2. But when the nanoparticle additive ratio was increased to 10%, the tensile strength value also increased to 1150 N/mm^2. For ATH-based samples 9% and for MDH-based samples 10% nano-sized $Mg(OH)_2$ addition limits were exceeded tensile strength values started to decrease.

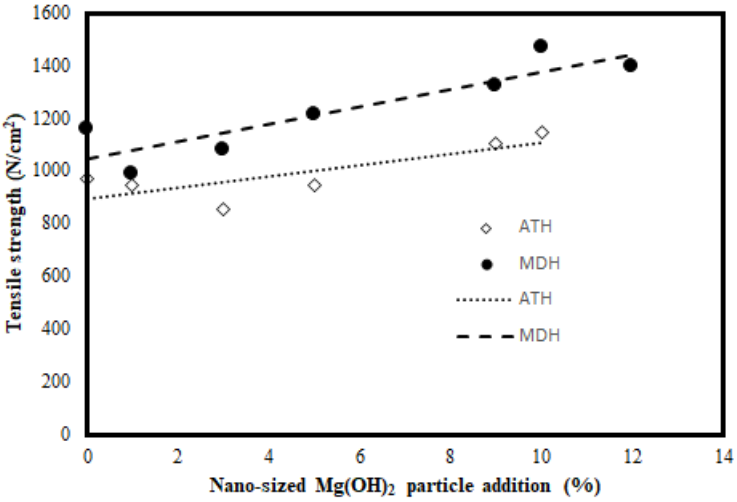

Figure 4.15 Nano-sized $Mg(OH)_2$ particles additive dependent tensile strength values

Table 4.7 Comparison of the positive effect of synthesized $Mg(OH)_2$ nanoparticles on LOI values in compounds with other studies in the literature.

EVA %	Flame retardant filler	Filler ratio %	Additive	Additive ratio %	LOI %	Reference
50	MDH	46	MWNT	4	37	Lei Ye et al., 2015
50	MDH	48	Nanoclay	2	35	Ynh-Yue Yen et al., 2012
50	ATH	48	Nanoclay	2	28	Ynh-Yue Yen et al., 2012
50	MDH	42.5	Layered Double Hydroxide	7.5	34	Guobing et al.,2016
40	ATH	54.5	Dibenzo Oxaphosphinic Acid (DOPA)	5.5	33.4	Li Yu et al., 2014
50	ATH	49.5	Hydroxy Silicon Oil	0.5	30.7	C.M.Jiao et al.,2009
45	MDH	52	Sepiolite	3	33.6	N.H.Huang et al., 2010
50	ATH	30	Melamine Cyanurate	20	27.5	Siyi Xu et al., 2021
50	MDH	45	MgAl LDH	5	33	Ding et al., 2011
40	MDH	50	Nano MDH	10	40.5	**This study**
40	ATH	51	Nano MDH	9	35.5	**This study**

As can be seen in Table 4.7, $Mg(OH)_2$ nanoparticles synthesized in this study increased the LOI values more than other additives in compounds containing both ATH and MDH. In this way, a compound with superior flame retardant property was formed.

Chapter 5

5. Conclusions and Future Prospects

5.1 Conclusions

In this thesis, it is aimed to improve the fire resistance property of Halogen Free Flame Retardant (HFFR) cable formulations using Aluminum hydroxide (ATH) as a flame retardant. Therefore, in the first part, the flame retardant performance of Magnesium hydroxide (MDH) instead of ATH was examined. In the second part, different raw materials were used for the synthesis of $Mg(OH)_2$ in nanoscale, and the most suitable raw material was selected as a result of structural and financial analyzes; in the third part, the synthesis was carried out at factory size and compared with the commercial product. In the last part, different amounts of nano-sized $Mg(OH)_2$ particles were added to the formulas using both ATH and MDH, and their effects on flame retardancy performances were investigated. Flame retardant properties were evaluated by investigating by limiting oxygen index values and vertical burning times. Important results for the characterization of samples are concluded as follows;

Comparison of flame retardant property of materials;

- First burning time results showed, both natural and synthetic $Mg(OH)_2$ had better flame retardant properties than $Al(OH)_3$. In the $Al(OH)_3$ based formula, the flame progression time to the marked 2 cm length took an average of 45 seconds, while this time was 75 seconds in synthetic $Mg(OH)_2$. (Figure 4.1)
- It was seen that the flame retardant property of synthetic $Mg(OH)_2$ was better than natural $Mg(OH)_2$. Synthetic $Mg(OH)_2$ (1,5 μm) improved the flame retardancy more than natural $Mg(OH)_2$ (3 μm) with its smaller particle size and higher purity.

With these results, it was thought that more effective flame retardant properties can be obtained by using nano-sized $Mg(OH)_2$.

Comparison of nano-sized particles synthesized from different salts;

- $MgCl_2$, $Mg(NO_3)_2$ and $MgSO_4$ salts were used to determine the magnesium containing raw material to be used in the synthesis. When the morphological structures of $Mg(OH)_2$ nanoparticles synthesized from these salts were examined, it was seen that the smallest and homogeneous grain structure was found in the product obtained from $Mg(NO_3)_2$. (Figure 4.3)
- Since the nano product to be produced will be used in factory-sized production, it was seen that the most advantageous product in terms of price is $MgSO_4$.
- By-product ammonium nitrate, resulting from the synthesis being performed was banned in Turkey because of its usage in producing of explosives. Due to widespread use of ammonium sulfate as a fertilizer, which is formed as a result of the reaction of $MgSO_4$ with NH_3 and the price advantage of $MgSO_4$, it was decided to make the factory scale synthesis using $MgSO_4$.

Comparison of commercial $Mg(OH)_2$ and factory-scale synthesized $Mg(OH)_2$ nano particles;

- When the SEM images were examined, it was seen that the commercial $Mg(OH)_2$ product consisted of multilayer hexagonal particles. The layers were agglomerated and had an integrated structure. It was seen that the factory-scale synthesized $Mg(OH)_2$ also consisted of nano-thick plates, but these plates were in a random structure without being uniformly agglomerated, thus creating much more surface area. (Figure 4.4)
- EDX and XRD results for both products showed that the purity of the materials was high.(Figure 4.5-4.6) As a result of the XRF analysis applied together with these, it was seen that the purity of commercial $Mg(OH)_2$ was higher. (Table 4.3) This is due to the low purity of the $MgSO_4$ salt used in the synthesis of the nano-sized material and the inadequacy of the filtration.
- The calculated theorical weight loss for $Mg(OH)_2$ is 30.86% and TG curves exhibit weight losses for both commercial and synthesized product is 38%.

- When the thermogravimetric analysis results were evaluated, it was seen that the decomposition of the commercial $Mg(OH)_2$ product occurred around 280°C, while the decomposition of the synthesized nano-sized $Mg(OH)_2$ product took place at 300°C. (Figure 4.8) This situation caused an increase in the initial ignition temperature of the material under the effect of heat, thus slowing the spreading of the flame.

Limiting Oxygen Index Values;

- As a result of the LOI values measurements, it was observed that the LOI values of the samples produced with $Mg(OH)_2$ were higher in the compound samples without nanoparticle additives. With this result, it was again seen that $Mg(OH)_2$ has better flame retardant property. (Figure 4.12)
- It was observed that nano-sized $Mg(OH)_2$ particle additions increased LOI values in both $Al(OH)_3$ and $Mg(OH)_2$ based compounds. The LOI value, which was 28.16% in Al(OH) based samples without nanoparticle additive, increased to 35.47% after 9% additive. Likewise, in $Mg(OH)_2$ based samples, the LOI value, which was 29.13% without nanoparticle additive, increased to 40.49% after 10% additive. However, the addition amount of nanoparticles negatively affected the LOI values after a certain limit. This is due to the fact that the nanoscale particles cannot be sufficiently mixed with the carrier polymer by the extruder. Nano powders that cannot be mixed with the polymer are thrown out from the discharge part of the extruder, so the LOI values of the compound with a high polymer ratio decrease. (pure EVA LOI value measured as 20.23%)

Vertical burning test results;

- In parallel with the LOI results, while the flame spreading rate is long in $Mg(OH)_2$ some compounds, it is short in $Al(OH)_3$ based compounds. (Figure 4.13) Nano-sized $Mg(OH)_2$ particle additives had a delayed effect on the spread time of the flame in both $Mg(OH)_2$ and $Al(OH)_3$ based samples. While this time was 24 hours for $Mg(OH)_2$ based sample with 1% nanoparticle additive, it increased to 55 seconds when the amount of additive was increased to 10%. It has been observed that when the nanoparticle addition limit, which is 9% for $Al(OH)_3$ based samples and 10% for $Mg(OH)_2$ based samples, is exceeded, the flame spread times are shortened due to the inability to achieve full mixing in the extruder.

Elongation and tensile strength tests;

- It was seen that the elongation values of the compound samples where MDH was used as a flame retardant were higher than the ATH based samples. (Figure 4.14)
- Elongation test results showed that as the amount of adding $Mg(OH)_2$ in nanoscale to $Al(OH)_3$ or $Mg(OH)_2$ based compounds increased, the elongation values decreased. In ATH and MDH based compound samples prepared without nano-sized $Mg(OH)_2$ additive, the elongation values, which were 135% and 170% respectively, decreased to 60% and 70% after 10% nano particle additive, respectively.
- In the first samples created with EVA polymer using 60% of ATH and MDH, it was observed that the tensile strength values as well as the elongation values in the MDH based samples were higher than the ATH based samples. (Approximately 950 N/mm^2 for MDH, approximately 1000 N/mm^2 for ATH) (Figure 4.15) As the ratio of adding nano-sized $Mg(OH)_2$ was increased, the tensile strength values of the materials also increased. After 10% nano sized $Mg(OH)_2$ addition, it increased to 1140 N/mm^2 in ATH based samples and 1468 N/mm^2 in MDH based samples.

The results of the thesis demonstrated that if MDH is used instead of ATH in cable insulations, better mechanical results, and flame retardancy are obtained. The disadvantage at this point is that ATH's price per kg is 0.765 € / kg (for ETİFINE 700), while MDH's price is 2.97 €/kg (for MAGNIFIN H5). Studies have shown that with the addition of $Mg(OH)_2$, which is produced in nano-size, to the formula currently used in production at a rate of 5%, there is an improvement of up to 8.6% in flame retardancy performance depending on LOI values. The addition of 5% nanoparticles both improved the flame retardant performance and ensured that the mechanical properties remained within acceptable limits. Thanks to the nanoparticle synthesis system build in the factory, it has been ensured that the nano powders are produced in the factory. As a result, nanoparticle doped high flame retardant cable insulation was produced in the factory environment.

5.2 Societal Impact and Contribution to Global Sustainability

Nano-sized flame retardants can be used not only in cable insulations, but also in all plastic-derived materials found in living environments. It can be used in much higher proportions in applications with no limitation of elongation values such as in cables. In this way, the burning effects of the plastic-derived items that cause the fire to spread are reduced, giving people more time to escape from the environment. But on the other hand, the flame retardant additive will cause some increase in the costs of the products.

By-products obtained according to the type of raw material to be used during the synthesis of nano-sized materials also find use in different areas. The ammonium sulphate obtained in this study is frequently used as a fertilizer in agriculture. By converting the by-products into commercial products and marketing them, the unit production costs of the nano-sized material can be reduced and a product needed in terms of agriculture can be supplied. In addition, with the use of this by-product, which is obtained as dissolved in water, in agriculture, both the penetration of the fertilizer to the plant will be accelerated and the irrigation function will be performed.

Nano-sized material synthesis by precipitation method can be easily enlarged to factory size without the need for huge costs. At this point, the most important issue is that the purity of the product to be synthesized to be used in cable insulation is high. Because as the material becomes purified, the negative effect of the cable insulation material on its mechanical properties decreases, thus, the amount of nano-sized material additives can be increased. In order to obtain a pure product, firstly the purity of the raw material to be used must be high, and the filtration processes must be done very well in the second stage. This situation causes the synthesis time of the material to be prolonged. The 60^{o}C temperature where the synthesis takes place can easily be reached by using the waste heat in the exhaust pipes in the factory. In this way, energy efficiency is achieved.

5.3 Future Prospects

- In areas where human population is much higher and fire risks are much greater, products with even more advanced flame retardant properties can be produced by using MDH + nano-sized $Mg(OH)_2$. Although the cost of this product is slightly higher, it will have much more effective flame retardant properties.
- By using much purer of the salt from which the nanoparticles are synthesized, and by using filter materials with smaller pores under the effect of vacuum, much higher purity nanoparticles can be obtained and thus the percentage of mixture in the compound can be increased.
- A new screw can be designed in cooperation with the Extruder company, which can provide much more nano powder mixture into the compound. In this way, instead of 60% micro-size powder in total, nano-sized and less powder can be used to produce cable insulations with much improved flame retardant property
- By using ATH in the formula and ensuring that nano-sized $Mg(OH)_2$ is coated only on the outer surface of the cable insulation, $Mg(OH)_2$, which is more effective in the first contact with the flame, can come to the fore.

BIBLIOGRAPHY

[1] Lu S.Y., Hamerton I., "Recent developments in the chemistry of halogen-free flame retardant polymers", Progress in Polymer Science, vol.27, Issue 8, pp. 1661-1712, (2002)

[2] Elektrik Kaynaklı Yangınlar ve Korunma Yöntemleri, www.emo.org.tr., (28.03.2021)

[3] Understanding cable fire, http://www.fppa.com.au/media/, (28.03.2021)

[4] Pang X.-Y, Tian Y., Weng M-Q., "Preparaton of expandable graphite with silicate assistant intercalation and its effect on flame retardancy of ethylene vinyl acetate composite", Polym.Compos., vol. 36, pp. 1407-1416, (2015)

[5] Sonnier R., Viretto A., Dumazert L., Longerey M., Buonomo S.,Gallard B., Longuet C.,Covedau F., Lamy R., Freitag A., "Fire retardant benefits of combining aluminum hydroxide and silica in ethylene vinyl acetate copolymer (EVA)", Polymer Degradation and Stability, vol. 128, pp. 228-236, (2016)

[6] F. Laoutid, M. Lorgouilloux, L. Bonnaud, D. Lesueur, P. Dubois, "Fire retardant behaviour of halogen-free calcium-based hydrated minerals", Polym. Degrad. Stab., vol. 136, pp. 89-97, (2007)

[7] Z. Li, B. Qu, "Flammability characterization and synergistic effects of expandable graphite with magnesium hydroxide in halogen-free flame-retardant EVA blends", Polym. Degrad. Stab., vol. 81, pp. 401-408, (2003)

[8] S. Bourbigot, M. Le Bras, R. Leeuwendal, K.K. Shen, D. Schubert, "Recent advances in the use of zinc borates in flame retardancy of EVA", Polym. Degrad. Stab., vol. 64, pp. 419-425, (1999)

[9] L. Ye, Q. Wu, B. Qu, "Synergistic effects and mechanism of multiwalled carbon nanotubes with magnesium hydroxide in halogen-free flame retardant EVA/MH/MWNT nanocomposites", Polym. Degrad. Stab., vol. 94, pp. 751-756 , (2009)

[10] Kiliaris P., Papaspyrides C.D., "Polymer Green Flame Retardants", Chapter 1-Polymers on Fire, pp. 1-43, (2014)

[11] Low voltage cables, 0.6/1 kV PVC Insulated, Round Steel Wire Armoured, multi-Core Cables With Copper Conductor, https://www.hes.com.tr, (13.02.2021)

[12] The electrical cable, definition and composition. https://www.icmesp.com, (20.07.2020)

[13] Cable and Wire Insulation Materials, https://www.awcwire.com (13.02.2021)

[14] Cable insulating materials, www.openelectrical.org, (13.02.2021)

[15] Popular Insulation Types, www.iewc.com, (14.02.2021)

[16] N. Hampton, R. Hartlein, H. Lennartsson, H. Orton, R. Ramachandran. "Long-life XLPE Insulated Power Cable", Georgia Tech Library, (2007)

[17] Etylene Propylene Rubber, www.en.wikipedia.org, (16.02.2021)

[18] Altarazi S., Omar Y. "Integration of Process Planning and Scheduling with Sequence Dependent Setup Time: A Case Study from Electrical Wires and Power Cable Industry", Springer Cham, (2015)

[19] N.D. Tran , N. Harada, T. Sasaki and T. Kikuchi. "Effect of a dielectric plasma annealing system at Atmospheric Pressure", Intechopen, (2012).

[20] Rodríguez-Alabanda Ó., Romero P.E., Molero E., Guerrero-Vaca G. "Analysis, Validation and Optimization of the Multi-Stage Sequential Wiredrawing Process of EN AW-1370 Aluminium", Metals, (2019)

[21] Zeroukhi, Y., Napieralska E., Komeza, K., Vega G., Morganti F., "3D electro-mechanical modeling of conductor after stranding and compacting process simulation". International Journal of Applied Electromagnetics and Mechanics, (2014)
[22] Compounding, www.extruders.leistritz.com, (21.02.2021)
[23] Thermo Fischer Scientific, why hot melt extrusion? www.thermofisher.com, (10.07.2021)
[24] Shrivastava A., "Plastics Processing, Introduction to Plastics Engineering", (2018)
[25] Fine driven payoff, www.swissline.ca, (20.02.2021)
[26] High speed flyer pay-offs, www.mobac.de, (20.02.2021)
[27] Extreme conditions require excellent cables, www.rosendahlnextrom.com, (20.02.2021)
[28] Extrusion lines, www.tecalsa.eu, (20.02.2021)
[29] Caterpillar, www.singcheer.com, (20.02.2021)
[30] Coiler, take-up, www.ritmindustry.com (21.02.2021)
[31] Global heat resistant polymer market, www.dailybizreport.com, (15.10.2020)
[32] Cantón R.F., Sanderson J.T., Nijmeijer S., Bergman A., Letcher R.J., van den Berg M, "In vitro effects of brominated flame retardants and metabolites on CYP17 catalytic activity: A novel mechanism of action", Toxicol Appl Pharmacol, (2006)
[33] Xu J., Liu X., Yang W., Lei N. L., Zhao J., Ma B., Kang C., "Influence of Montmorillonite on the Properties of Halogen-Antimony Flame Retardant Polypropylene Composites", Polymer Composites, (2018)
[34] How Flame Retardant Systems Work In Plastics., www.rtpcompany.com, (20.10.2020)
[35] FR mechanisms, www.fr.polymerinsights.com, (22.10.2020)
[36] Novel halogen free epoxy resin for high performance electronic applications, www.slideplayer.com, (22.10.2020)
[37] Extrusion lines for cable manufacturing, www.expometals.net, (25.10.2020)
[38] Ethylene-vinyl acetate, www.en.wikipedia.org, (24.10.2020)
[39] Elvax Thermal Properties, www.dupont.com, (24.10.2020)
[40] Ethylene vinyl acetate copolymer (EVA), www.polymerdatabase.com, (24.10.2020)
[41] Flame-retardant Mechanism of Magnesium Hydroxide, www.medium.com, (24.10.2020)
[42] V.Koncar. "Smart Textiles for in Situ Monitoring of Composites", Woodhead Publishing, (2019)
[43] Van Krevelen D.W., Te Nijenhuis K., "The Correlation with Chemical Structure; Their Numerical Estimation and Prediction from Additive Group Contributions", (2009)
[44] Fire Retardant Adhesives – 4 Crucial Properties, www.permabond.com, (21.03.2021)
[45] Process, www.magnifin.com, (21.03.2021)

CURRICULUM VITAE

2002 – 2008	B.Sc., Mechanical Engineering, Akdeniz University, Antalya, TURKEY
2008 – 2010	Mechanical Works Chief, Park View Office Tower, Almaty, KAZAKHSTAN
2011 – 2012	Enamelled Wire Production Engineer, Hes Kablo, Kayseri, TURKEY
2012 – Present	Enamelled Wire Production Chief, Hes Kablo, Kayseri, TURKEY
2018 – Present	M.Sc., Advanced Materials and Nanotechnology, Abdullah Gül University, Kayseri, TURKEY